

RESEARCH ARTICLE



Role for the liver X receptor agonist 22-ketositosterol in preventing disease progression in an Alzheimer's disease mouse model

Nikita Martens^{1,2} | Na Zhan^{1,3,4} | Sammie C. Yam¹ | Marcella Palumbo⁵ | Lorenzo Pontini⁶ | Frank P. J. Leijten¹ | Leonie van Vark-van der Zee¹ | Gardi Voortman¹ | Silvia Friedrichs⁴ | Albert Gerding⁷ | Maura Marinozzi⁶ | Johan W. Jonker⁷ | Folkert Kuipers^{7,8} | Dieter Lütjohann⁴ | Tim Vanmierlo^{1,2,9} | Monique T. Mulder¹

¹Department of Internal Medicine, Section Pharmacology and Vascular Medicine, Erasmus University Medical Center, Rotterdam, The Netherlands

²Department of Neuroscience, Biomedical Research Institute, Faculty of Medicine and Life Sciences, Hasselt University, Hasselt, Belgium

³Key Laboratory of Marine Drugs, Chinese Ministry of Education, School of Medicine and Pharmacy, Ocean University of China, Qingdao, China

⁴Institute of Clinical Chemistry and Clinical Pharmacology, University Hospital Bonn, Bonn, Germany

⁵Department of Food and Drug, University of Parma, Parma, Italy

⁶Department of Pharmaceutical Sciences, University of Perugia, Perugia, Italy

⁷Department of Pediatrics, Section of Molecular Metabolism and Nutrition, University of Groningen, University Medical Center Groningen, Groningen, The Netherlands

⁸European Research Institute for the Biology of Ageing (ERIBA), University of Groningen, University Medical Center Groningen, Groningen, The Netherlands

⁹Department Psychiatry and Neuropsychology, Mental Health and Neuroscience Institute, Maastricht University, Maastricht, The Netherlands

Correspondence

Monique T. Mulder, Department of Internal Medicine, Section Pharmacology and Vascular Medicine, Erasmus University Medical Center, 3015 CN Rotterdam, The Netherlands.
Email: m.t.mulder@erasmusmc.nl

Funding information

This research was funded by the Dutch Research Council (NWO-TTW) (#16437), the Alzheimer Nederland and Alzheimer Forschung Initiative (#WE.03-2018-06 AN, #WE.03-2022-06, #WE.15-2021-08, #AFI-22034CB), the Ministry of University and Research (MUR), National Recovery and Resilience Plan (NRRP), project MNESYS (PE0000006) and a multiscale integrated approach to the study of the nervous system in health and disease (DN. 1553 11.10.2022).

Background and Purpose: Liver X receptors (LXRs) are promising therapeutic targets for alleviating Alzheimer's disease (AD) symptoms. We assessed the impact of the semi-synthetic LXR agonist 22-ketositosterol on disease progression in an AD mouse model.

Experimental Approach: From 5.5 months of age, APP^{swe}PS1 Δ E9 (AD) mice and wild-type (WT) littermates received a regular or 22-ketositosterol-supplemented diet (0.017% w/w). Cognition was assessed with object location and recognition tasks and a spontaneous alternation Y-maze test. Amyloid β was quantified using immunohistochemistry (IHC) and enzyme-linked immunosorbent assay (ELISA), microglia (Iba1, CD68) and astrocyte (GFAP) markers using IHC. Sterols were determined in food, serum, liver and cerebellum.

Key Results: 22-Ketositosterol activated both liver X receptors- α and - β and promoted cholesterol efflux in cell cultures. Diet supplementation with 22-ketositosterol

Abbreviations: A β , Amyloid β ; AD, Alzheimer's Disease; ApoA-I, Apolipoprotein A-I; CD68, Cluster of Differentiation 68; FCS, Foetal Calf Serum; GOS2, G0/G1 Switch Gene 2; GFAP, Glial Fibrillary Acidic Protein; Iba1, Ionized Calcium-Binding Adaptor Molecule 1; LXR, Liver X Receptor; OLT, Object Location Task; ORT, Object Recognition Task; SREBP, Sterol Regulatory Element-Binding Protein; VLDL, Very-Low-Density Lipoprotein; 24-OHC, 24-Hydroxycholesterol; 27-OHC, 27-Hydroxycholesterol; 7 α -OHC, 7 α -Hydroxycholesterol.

This is an open access article under the terms of the [Creative Commons Attribution](https://creativecommons.org/licenses/by/4.0/) License, which permits use, distribution and reproduction in any medium, provided the original work is properly cited.

© 2025 The Author(s). *British Journal of Pharmacology* published by John Wiley & Sons Ltd on behalf of British Pharmacological Society.

prevented a decline in the performance of APPswePS1ΔE9 mice in the object location task but not in the other two tasks. Without affecting amyloid β deposition, 22-ketositosterol decreased microglia (Iba1, CD68) and astrocyte (GFAP) markers in the cortex and hippocampus of APPswePS1ΔE9, suggesting potential anti-inflammatory effects. No lipid accumulation was detected in the liver or serum upon 22-ketositosterol supplementation.

Conclusions and Implications: Diet supplementation with 22-ketositosterol prevented the decline in spatial memory of APPswePS1ΔE9 mice. Our data suggest therapeutic benefits of 22-ketositosterol possibly by enhancing cholesterol efflux and mitigating inflammatory responses, without inducing hepatosteatosis or hypertriglyceridemia.

KEYWORDS

Alzheimer's disease, cholesterol metabolism, liver X receptors, oxysterols

1 | INTRODUCTION

Alzheimer's disease (AD) is the most prevalent form of dementia. It is a progressive neurodegenerative disorder characterised by a complex interplay of genetic and environmental factors. Neuropathological characteristics of AD are **amyloid β (A β)** plaques, aggregated hyperphosphorylated tau, progressive loss of synapses and neurons, and neuroinflammation (Blennow et al., 2006; Hardy & Selkoe, 2002). Emerging research demonstrates an imbalance in **cholesterol** homeostasis in the brain of AD patients, which is thought to contribute to synaptic and neuronal loss (Marchi et al., 2019; Yassine et al., 2016). The global increase in the prevalence of AD, driven by the ageing population, has underscored the urgent need for the discovery of novel therapeutic targets and underlying mechanisms of AD.

Liver X receptors α and β (LXR α/β ; NR1H3/NR1H2), nomenclature as agreed by the International Union of Pharmacology (IUPHAR)/BPS Subcommittee on Nuclear Hormone Receptors (Alexander et al., 2023; McDonnell & Safi, 2023), have emerged as promising therapeutic targets for AD. LXRs are ligand-activated transcription factors with a pivotal role in regulating lipid and sterol metabolism and reducing inflammatory responses (Moutinho & Landreth, 2017; Xu et al., 2021; Zelcer & Tontonoz, 2006). In AD, there is an excessive activation of microglia and astrocytes, which contributes to the neuroinflammatory component of AD-related pathology. Besides driving cholesterol efflux, LXR activation can suppress the release of pro-inflammatory cytokines by microglia and astrocytes, thereby mitigating their reactivity (Mouzat et al., 2019; Sandoval-Hernández et al., 2015; Zelcer et al., 2007). By inhibiting the inflammatory response of glial cells and promoting cholesterol efflux, activation of LXR has been demonstrated to beneficially impact the cognitive performance in AD mouse models (Donkin et al., 2010; Jiang et al., 2008; Moutinho & Landreth, 2017; Riddell et al., 2007; T. Vanmierlo et al., 2011), reinforcing their neuroprotective potential.

We have recently reported that the LXR agonist 24(S)-saringosterol prevents cognitive decline in a mouse model of AD

What is already known?

- Liver X receptors (LXRs) are promising therapeutic targets for the alleviation of Alzheimer's disease (AD) symptoms.

What does this study add?

- Our data suggest therapeutic benefits of 22-ketositosterol possibly by enhancing cholesterol efflux and mitigating inflammation.

What is the clinical significance?

- 22-Ketositosterol bypasses lipid accumulation, unlike most synthetic liver X receptors agonists, warranting further therapeutic research.

(Martens et al., 2021). Our data indicate that the anti-inflammatory effects of 24(S)-saringosterol may have contributed to the cognitive enhancement. In contrast with previously used synthetic pan LXR agonists (Donkin et al., 2010; Jiang et al., 2008; Riddell et al., 2007; T. Vanmierlo et al., 2011), no adverse effects, such as hepatosteatosis and hypertriglyceridemia (Grefhorst et al., 2002; Repa et al., 2000; Schultz et al., 2000) were observed. Because these adverse effects have been attributed to the activation of LXR α (Quinet et al., 2006; Schultz et al., 2000; Zhang et al., 2012), compounds selectively activating LXR β may provide opportunities for application in treatment. Alternatively, LXR-activating oxysterols that do not induce the lipogenesis pathway (Radhakrishnan et al., 2004), such as 24(S)-saringosterol, are promising therapeutic candidates. From a small library of

ergosterol and stigmasterol derivatives that were designed as potential LXR agonists, the stigmastane derivative 22-ketositosterol (PFM018 in reference Marinozzi et al., 2017) was identified as a preferential LXR β agonist. 22-Ketositosterol was found to induce cholesterol efflux-related genes but hardly lipogenic genes (Marinozzi et al., 2017). Here we assess the potential of 22-ketositosterol in ameliorating disease progression in an AD mouse model.

2 | METHODS

2.1 | Cell cultures

Immortalised HEK293 cells (Cat# CB-85120602; RRID: CVCL_0045; Merck, Amsterdam, The Netherlands), human astrocytoma cells (CCF-STTG1; Cat# CB-90021502; RRID: CVCL_1118; Merck), human neuroblastoma cells (SH-SY5Y; Cat# CRL-2266; RRID: CVCL_0019; American Type Culture Collection [ATCC]) and human microglia cells (CHME3; a kind gift from prof. Dr. M. Tardieu, Université Paris-Sud, France) were used for the reporter assays. CCF-STTG1 cells (Merck) and primary human astrocytes (HA; #1800, ScienCell, Carlsbad, CA, USA; kindly provided by Prof. dr. B. Broux [Biomedical Research Institute, Faculty of Medicine and Life Sciences, Hasselt University, Belgium]) were used for the gene expression experiments; human hepatic HepG2 cells (kindly provided by professor M. Ruscica, Department of Pharmacological and Biomolecular Sciences, University of Milan, Italy) for the analysis of cholesterol efflux, cholesterol and cholesterol precursors, and human monocyte-derived macrophages (THP-1 cells [Cat# 88081201; RRID: CVCL_0006] from European Collection of Authenticated Cell Cultures [ECACC]; purchased from Sigma-Aldrich, St. Louis, MO, USA) were used for the analysis of cholesterol efflux. The HEK293, CCF-STTG1, SH-SY5Y and CHME3 cells were cultured in DMEM/F-12 medium supplemented with 10% heat-inactivated foetal calf serum (FCS) and 1% 10,000 U penicillin per 10,000 μg streptomycin ml^{-1} at 37 °C and 5% CO_2 . The HepG2 cells were cultured in MEM medium with Earle's salts supplemented with 1% penicillin/streptomycin, 1% L-Glutamine, 1% sodium pyruvate (Na-Pir), 1% non-essential amino acids solution (NEAA) and 10% FCS. The THP-1 cells (from ECACC; purchased from Sigma-Aldrich, St. Louis, MO, USA) were cultured in RPMI 1640 medium supplemented with HEPES, 0.05 mM β -mercaptoethanol, 0.5% v/v gentamycin, 0.25 g ml^{-1} w/v glucose, 1 mM Na-pir and 10% v/v FCS. THP-1 cells were seeded for 72 h in the presence of 100 ng ml^{-1} phorbol 12-myristate 13-acetate (PMA) to allow differentiation into macrophages. Both HepG2 (400,000 cells per well) and THP-1 cells (500,000 cells per well) were seeded in 24-well plates at 37 °C and 5% CO_2 . The primary human astrocytes were cultured at 37 °C and 5% CO_2 in astrocyte medium (AM, #1801, ScienCell, Carlsbad, CA, USA) supplemented with 2% FCS (#0010, ScienCell, Carlsbad, CA, USA), 1% astrocyte growth supplement (AGS, #1852, ScienCell) and 1% penicillin/streptomycin (#0503, ScienCell, Carlsbad, CA, USA) in flasks coated with poly-L-lysine (PLL; 1 mg ml^{-1} , Cat. #0403, ScienCell, Carlsbad, CA, USA). The human astrocytes were seeded in T-75

flasks at a density of 3.75×10^6 cells per flask. Once a confluence level of 70% was reached, the medium was changed every other day until 90% confluence was achieved.

2.2 | LXR reporter assay

LXR activation was determined in a cell-based reporter assay previously described by Zwarts et al. (2019). 1.0×10^6 cells were plated in T-25 culture flasks and transfected with 1000 ng of pcDNA3.1/V5H6 vector containing clones of the full-length cDNAs for the murine nuclear receptors LXR α or LXR β , 1000 ng of vector encoding **retinoid X receptor- α gene (Rxra)** and 4000 ng of vectors encoding **LXR α gene (Nr1h3)** using FuGENE[®] 6 reagent (Promega, Leiden, The Netherlands). Cells transfected with 4000 ng of the liver X receptor response element (LXRE)-containing vector and 2000 ng of an empty pcDNA3.1/V5-HisA vector (Invitrogen, Carlsbad, CA, USA) or 2000 ng of the RXR α -containing vector served as controls. All cells were co-transfected with Renilla (1000 ng, pRL TK-Renilla) to normalise for variations in transfection efficiency.

The transfected cells were seeded in a 96-well luminescence plate and after 24 h incubated for 24 h in phenol red-free DMEM/F-12 medium with 22-ketositosterol (2, 5 or 10 μM), the LXR α/β agonist **T0901317** (1 μM ; #293754-55-9) or ethanol. The cells were lysed with lysis buffer, and the Firefly and Renilla luminescent signals were measured using the Dual-Luciferase[®] Reporter assay system (Promega) and a Victor X4 plate reader (PerkinElmer, Groningen, The Netherlands). The relative receptor activity was defined as the ratio of Firefly luminescence to Renilla luminescence. The fold change was defined as the ratio of the relative receptor activity of 22-ketositosterol- or agonist-exposed cells to the relative receptor activity of ethanol-exposed cells. The experiments were performed three times in triplicate.

2.3 | Quantitative real-time PCR

CCF-STTG1 cells and primary human astrocytes were incubated for, respectively, 24 and 48 h with 22-ketositosterol or its solvent ethanol after which the cells were washed with cold phosphate-buffered saline. RNA was isolated from cells or homogenised liver tissue using Trizol (Thermo Fisher Scientific) and reverse transcribed to cDNA using the Maxima H Minus First Strand cDNA Synthesis Kit with dsDNase (Thermo Fisher Scientific), according to the manufacturer's instructions. Quantitative real-time PCR (qPCR) was conducted in duplicate with 10 ng cDNA on a CFX384 Thermal Cycler (Bio-Rad Laboratories) using the PowerTrack[™] SYBR Green Master Mix (Applied Biosystems) and the following cycling conditions: 95 °C for 2 min and 40 cycles of 95 °C for 15 s and 60 °C for 60 s. Intron-spanning primers were designed with Primer-BLAST. The primer sequences are listed in Table 1. The relative quantification of gene expression was accomplished with the comparative Ct method ($\Delta\Delta\text{CT}$). The data were normalised to stable reference genes (*ACTB*,

TABLE 1 Nucleotide sequences of primers.

Cell cultures		
Gene	Gene name	Primer sequence
ABCA1	ATP binding cassette subfamily A member 1	F: TCTCTGTTCCGGCTGAGCTAC R: TGCAGAGGCATGGCTTTAT
ABCG1	ATP binding cassette subfamily G member 1	F: GGTCGCTCCATCATTGACAC R: GCAGACTTTTCCCCGTACA
ACTB	Actin beta	F: CTCCTGGAGAAGAGCTACG R: GAAGGAAGGCTGGAAGAGTG
APOE	Apolipoprotein E	F: ACCCAGGAAGTGGGGC R: CTCCTTGGACAGCCGTG
B2M	Beta-2-microglobulin	F: CTCCTGGCCTTAGCTGTG R: TTTGGAGTACGCTGGATAGCCT
HPRT1	Hypoxanthine phosphoribosyltransferase 1	F: TGACACTGGCAAACAATGCA R: GGTCCTTTTACCAGCAAGCT
SDHA	Succinate dehydrogenase complex flavoprotein subunit A	F: TGGGAACAAGAGGGCATCTG R: CCACCACTGCATCAAATTCATG
TBP	TATA-box binding protein	F: CACGAACCACGGCACTGATT R: TTTTCTTGCTGCCAGTCTGGAC
YWHAZ	Tyrosine 3-monooxygenase/tryptophan 5-monooxygenase activation protein zeta	F: ACTTTTGGTACATTGTGGCTTCAA R: CCGCCAGGACAAACCAGTAT
Liver samples (mouse)		
Acaca	Acetyl-CoA carboxylase alpha	F: CTCACAGCGTACAACACCG R: TGGGGATGTTCCCTCTGTTTG
Actb	Actin beta	F: TTCTTGGGTATGGAATCCTGTGG R: GTCCTTACGGATGTCAACGTCAC
B2m	Beta-2-microglobulin	F: CATGGCTCGCTCGGTGACC R: AATGTGAGGCGGGTGAAGTGA
Fasn	Fatty acid synthase	F: GGCCCTCTGTTAATTGGCT R: GGGATAACAGCACCTTGGTCA
G0s2	G0/G1 switch 2	F: CCCGAGGGAAGCTAGTGAAG R: GCTGCACACCGTCTCAACT
Hprt1	Hypoxanthine phosphoribosyltransferase 1	F: CCTAAGATGAGCGCAAGTTGAA R: CCACAGGACTAGAACCTGTAA
Scd1	Stearoyl-CoA desaturase 1	F: GGCCTGTACGGGATCATACTG R: GGTCATGTAGTAGAAAATCCCGAAG
Sdha	Succinate dehydrogenase complex flavoprotein subunit A	F: CTTGAATGAGGCTGACTGTG R: ATCACATAAGCTGGTCCTGT
Srebf1	Sterol regulatory element binding transcription factor 1	F: GCCATCGACTACATCCGCTT R: CAGGTCCTTCAGTGATTTGCTTT

B2M, HPRT1 and SDHA) and expressed as fold change relative to ethanol-exposed cells or the vehicle-treated WT mice. Although the gene expression levels in cells were assessed in three to four individual experiments ($n < 5$), the exploratory data clearly demonstrated that 22-ketositosterol increased the expression of the selected genes (ABCA1, ABCG1 and APOE) in a dose-dependent manner. Therefore, no additional tests were required.

2.4 | Cholesterol efflux assay

Cellular cholesterol efflux was evaluated in HepG2 and THP-1 cells by a standardised radio-isotopic technique as described previously (Adorni et al., 2023; Zhan et al., 2023). The cells were labelled with

1,2-³H(N)]-cholesterol (PerkinElmer, Waltham, MA, USA) at 2 $\mu\text{Ci ml}^{-1}$ in the presence of 1% FCS-containing MEM or RPMI and 2 $\mu\text{g ml}^{-1}$ Sandoz 58-035, which is an inhibitor of acyl-coenzyme A and **cholesterol acyltransferases (ACAT)** that prevents the accumulation of cholesteryl esters. Cell monolayers were then, in the presence of the ACAT inhibitor, equilibrated for 20 h in 0.2% bovine serum albumin (BSA)-containing medium supplemented with ethanol, 1 μM of T0901317 or 22-ketositosterol (1.25, 2.5 or 5.0 μM). Cholesterol efflux was induced by 4 (in HepG2) or 6 h (in THP-1) of incubation with 10 $\mu\text{g ml}^{-1}$ of lipid-free human apolipoprotein A-I (ApoA-I), 12.5 $\mu\text{g ml}^{-1}$ of human high-density lipoprotein (HDL) or 2% (v/v) serum of a pool of normolipidemic subjects. Sera were slowly thawed in ice immediately prior to this procedure to prevent remodelling of the lipoproteins. The cholesterol efflux was expressed as the ratio

of radiolabelled cholesterol released into the medium over the total radioactivity incorporated by cells (Turri et al., 2023).

2.5 | Intracellular sterols quantification

CCF-STTG1, SH-SY5Y and HepG2 cells were plated and incubated for 24 h with 22-ketositosterol (1.25 μM) or ethanol as control. Sterols were extracted from the cells, and the concentrations of 22-ketositosterol; cholesterol; and cholesterol precursors lanosterol, desmosterol and lathosterol were determined using gas chromatography–mass spectrometry (GC–MS), as described previously (Lütjohann et al., 2002; Mackay et al., 2014). Sterols and oxysterols were extracted by cyclohexane after saponification and neutralisation. The solvents were evaporated and the sterols and oxysterols in the residue were derivatised to mono-, di- or trimethylsilyl (TMSi) ethers by adding 1 ml TMSi-reagent (pyridine-hexamethyldisilazane-trimethylchlorosilane; 9:3:1, v/v/v) and incubated for 1 h at 64°C. The solvents were evaporated under nitrogen at 65°C. The residue was dissolved in 160 μl *n*-decane. Around 80 μl of the solution was transferred into micro-vials for gas–liquid chromatographic–mass spectrometric (GC–MS) analysis of cholesterol precursors, metabolites and phytosterols. The remaining 80 μl was diluted with 400 μl *n*-decane for analysis of cholesterol by gas chromatography–flame ionisation detection. TMSi-ether of epicoprostanol was measured at mass-to-charge ratio (*m/z*) 370 (M^+ -OTMSi), lathosterol at *m/z* 458 (M^+), desmosterol at *m/z* 441 (M^+ -CH₃), lanosterol at *m/z* 393 (M^+ -OTMSi-CH₃) and 22-ketositosterol at *m/z* 500 [M^+]. The concentrations of lathosterol, desmosterol and lanosterol were calculated from the standard curves using epicoprostanol (10 μl from a stock solution epicoprostanol in cyclohexane; 100 $\mu\text{g ml}^{-1}$) as an internal standard and using GC–MS–selected ion monitoring (SIM). The concentration of cholesterol was calculated by one-point calibration using 5 α -cholestane as an internal standard using GC–FID. The peak area of cholesterol is divided by the peak area of 5 α -cholestane and multiplied by the amount of 5 α -cholestane added to the sample (50 μg).

2.6 | Animals and diet

The 22-ketositosterol-treated mice presented in this report were included in the experiment detailed in Martens et al. (2024). In that experiment, a shared control group comprised mice receiving a non-supplemented, vehicle diet. This control group was utilised for comparison across both treatments. All animal studies are reported in compliance with the ARRIVE guidelines (Percie du Sert et al., 2020) and with the recommendations made by the *British Journal of Pharmacology* (Lilley et al., 2020).

Male APPswePS1 ΔE9 (AD) and wild-type (WT) littermates were obtained by backcrossing male APPswePS1 ΔE9 mice (RRID: MGI:2384432; The Jackson Laboratory, Bar Harbor, ME, USA) with female C57BL6/J mice (Envigo, Horst, The Netherlands). The animals

were housed in a conventional animal facility at Hasselt University in open cages with sufficient environmental enrichment and had *ad libitum* access to food and water. The animals were kept at an inverted 12 h light/12 h dark cycle. The behaviour experiments were performed during the dark phase of the cycle. The mice were housed individually throughout the entire experiment. The animal procedures were approved by the ethical committee of Hasselt University (protocol ID202036) and were in accordance with institutional guidelines. From 5.5 months of age, the mice were assigned to two treatment groups using a balanced distribution approach, ensuring comparable baseline performance in cognitive tests across the groups. For a period of 12 weeks, one group received standard chow (VRF1, Sniff Spezialdiäten GmbH, Soest, Germany) (APPswePS1 ΔE9 *n* = 13, C57BL6/J *n* = 13), and the other group received chow supplemented with 22-ketositosterol (APPswePS1 ΔE9 *n* = 13, C57BL6/J *n* = 13). The sample size was determined by a power calculation based on data from a prior study (Bogie et al., 2019) (α = 0.05, power = 0.80). The mice were assigned to the treatment groups using a balanced distribution approach, ensuring groups of equal size and comparable baseline performance in cognitive tests across all groups. 22-Ketositosterol was mixed through the standard chow and dried to pellets overnight at 40°C. After drying, the supplemented chow contained 166 $\mu\text{g g}^{-1}$ (0.017% w/w) 22-ketositosterol. This dose was based on previous experiment where animals were supplemented with 24(S)-saringosterol (Martens et al., 2021). The non-supplemented, vehicle, chow did not contain 22-ketositosterol. The body weight of the animals was recorded on a weekly basis. When mice exhibited more than 20% weight loss compared to the highest measured value, humane endpoints were reached, and the animal would have been euthanized. However, none of the animals in the study reached these endpoints.

2.7 | Cognitive tests

The object recognition task (ORT), object location task (OLT) and spontaneous alternation Y-maze test were performed to evaluate the object memory, spatial memory and spatial working memory, respectively. Prior to the cognitive tests at baseline, the animals were habituated to the arena and study objects that were used for the cognitive tests. A functional memory of WT and APPswePS1 ΔE9 mice at baseline was confirmed with the OLT (Figure S1). After the baseline tests, diet supplementation was initiated. At the end of the treatment period, the ORT, OLT and Y-maze were performed as previously described (Bogie et al., 2019; Martens et al., 2021).

2.7.1 | Object recognition task (ORT) and object location task (OLT)

For the ORT and OLT, the animals were exposed for 4 min to two similar objects after which they were placed back in their home cage. After 2.5 h (ORT) or 5 h (OLT), a second trial of 4 min was performed. During this second trial, the animals were exposed to either one

familiar object from trial 1 and one novel object (ORT) or to the two objects from trial 1 of which one object was moved to another location (OLT). The time the animals spent exploring each object during the two trials was recorded manually by two researchers who were blinded to the experimental groups. As a measure of object memory (ORT) and spatial memory (OLT), a discrimination index (D2) was calculated for trial 2: (exploration time of novel [ORT] or displaced [OLT] object)–(exploration time of familiar [ORT] or stationary [OLT] object)/(total exploration time). D2 values above 0 demonstrate a preference for the novel/displaced object. To prevent olfactory cues, the arena and study objects were cleaned with 70% ethanol prior to each trial. Animals that did not reach a minimum of 4 s of exploration in one of the trials and extreme values, as determined by Dixon's exclusion principles (Dixon, 1950, 1951), were excluded from further analyses.

2.7.2 | Spontaneous alternation Y-maze test

The spontaneous alternation Y-maze test was conducted with a maze with three arms of equal length, separated with an angle of 120°. The animals were placed in one of the arms and explored the maze for 2 min. Each arm entry was recorded manually. An arm entry requires that all four limbs of the animal are within the arm. As a measure of spatial working memory, the percentage of alternations was calculated as follows: number of alternations/(total number of entries – 2) * 100. The number of alternations was defined as the subsequent entry of the three different arms. Percentages of alternation above 50% are considered an indication of a well-functional working memory. The Y-maze was cleaned with 70% ethanol prior to each trial to prevent olfactory cues. Extreme values, as determined by Dixon's exclusion principles (Dixon, 1950, 1951), were excluded from further analysis.

2.8 | Tissue sample preparation

The animals were euthanized to obtain tissues for further analysis. The animals were anaesthetised via intraperitoneal (i.p.) injection of pentobarbitone (Dolethal; Vetoquinol, Aartselaar, Belgium) (200 mg kg⁻¹ body weight) followed by a cardiac puncture to obtain a blood sample. The blood samples were collected in a regular Eppendorf then centrifuged for 5 min at 4000 g and 4°C to obtain serum, which was stored at –80°C until further use. Prior to the isolation of tissue samples, we performed transcardiac perfusion with Heparin-phosphate-buffered saline (PBS). Brains were isolated and divided into the cerebellum and the remaining two hemispheres. The right cerebellum was snap-frozen and cryopreserved for sterol analysis. The cortex was isolated from the right hemisphere, snap-frozen and cryopreserved for an enzyme-linked immunosorbent assay (ELISA) of Aβ₄₂. The left hemisphere was fixed in formalin and embedded in paraffin for immunohistochemistry. The liver was isolated, snap-frozen and stored at –80°C for measurement of sterols and triglycerides. Part of the left liver lobe was embedded in OCT mounting medium (VWR

International, Leuven, Belgium) for cryosection and subsequent staining of neutral lipids.

2.9 | Sterol measurements in tissues

The tissue samples were spun in a speed vacuum dryer and weighted to relate the sterol concentrations to the dry weight of the samples. The sterols were extracted from the tissues and their concentrations were determined by GC–MS as previously described (Lütjohann et al., 2002; Mackay et al., 2014).

2.10 | Immunohistochemistry

All the Immuno-related procedures used comply with the recommendations made by the *British Journal of Pharmacology* (Alexander et al., 2018).

The left hemispheres of the animals were fixed in 10% formalin and embedded in paraffin using a Thermo Scientific Excelsior ES Tissue Processor (Thermo Fisher Scientific, Waltham, MA, USA) in increasing concentrations of ethanol (70% for 1 h, 80% for 1 h, 95% for 1 h, 100% for 1.5 h), xylene (1.5 h) and paraffin wax (2 h at 60°C). The embedded hemispheres were sectioned with an HM 330 Motorised Rotary Microtome (Microm GmbH, Heidelberg, Germany) to obtain 5-µm sections. The sections were mounted on glass slides, air-dried overnight at 37°C and stored at room temperature (RT) until further use.

Immunohistochemistry was performed as described previously (Martens et al., 2021). The sections were deparaffinised by incubation in xylene for 10 min, followed by incubation in decreasing concentrations of ethanol (100% for 6 min, 96% for 3 min, 70% for 3 min). After washing the sections in Tris-buffered saline (TBS) per 0.3% Triton X-100, they were incubated in 10-mM citrate buffer (pH 6.0) for 10 min at 100°C. After cooling down, the sections were washed with PBS, incubated in 3% H₂O₂/methanol for 10 min at RT and rinsed for 5 min with TBS/0.3% Triton X-100. The sections were incubated with blocking solution (5 v/v% bovine serum albumin in TBS/0.3% Triton X-100) for 1 h at RT after which the sections were incubated overnight at 4°C with 150 µl of the primary antibody (anti-Aβ: recombinant mouse Aβ antibody [IgG1], clone 3D6, Creative Biolabs Cat# TAB-0809CLV; RRID: AB_3111798, provided by P. Martinez-Martinez and M.R. Losen [School for Mental Health and Neuroscience Institute, Maastricht University, Maastricht, The Netherlands] [1:8000]; polyclonal rabbit Iba1 antibody (IgG): Cat# 019-19741; RRID: AB_839504; Wako Chemicals USA, Inc., Richmond, VA, USA [1:1000]; monoclonal rat Cluster of Differentiation 68 (CD68) antibody [IgG2a]: Cat# MCA1957; RRID: AB_322219; Bio-Rad Laboratories Inc., Hercules, CA, USA [1:100]; and polyclonal rabbit GFAP antibody: Cat# Dako-Z0334; RRID: AB_10013382; Agilent Technologies, Glostrup, Denmark [1:2000]). The sections were washed with TBS/0.3% Triton X-100, followed by a 30-min incubation with 150 µl of biotinylated secondary antibodies: goat anti-human IgG antibody

(H + L, BA-3000, [RRID:AB_2336148](#); 1:500), goat-anti-rabbit IgG antibody (H + L, BA-1000, [RRID:AB_2313606](#); 1:500), goat anti-rat IgG antibody (H + L, BA-9400, [RRID:AB_2336202](#); 1:200) and goat anti-rabbit IgG antibody (H + L, BA-1000, [RRID:AB_2313606](#); 1:500) (Vector Laboratories, Burlingame, CA, USA) for staining of A β , Iba1, CD68 and GFAP, respectively. The antibody dilutions were freshly made from their stocks. After washing with TBS/0.3% Triton X-100, avidin-biotin complex reagent (ABC kit, Vector Laboratories, Newark, CA, USA) was added to the sections and incubated for 30 min at RT. The avidin-biotin complex reagent was washed away, and diaminobenzidine (ImmPACT DAB, Vector Laboratories, Newark, CA, USA) was added. Once the staining was visible, the slides were dipped in distilled water (dH₂O) and dehydrated by incubation in 70% ethanol (1 min), 100% ethanol (1 min) and xylene (1 min). The coverslips were mounted with Entellan. Images of the sections were acquired using a Nanozoomer 2.0 HT slide scanner (Hamamatsu Photonics K.K., Shizuoka, Japan).

The surface area of the A β staining was quantified using Fiji ImageJ software by defining the pixel intensity of the staining in the total cortical or hippocampal area. The surface area of Iba1, CD68 and GFAP staining was determined with Trainable Weka Segmentation in ImageJ (Arganda-Carreras et al., [2017](#)).

2.11 | A β ₄₂ isolation and quantification (ELISA)

The cortex of the right hemisphere of APP^{swePS1 Δ E9} mice was homogenised in TBS/0.1% Triton X-100 with 2% complete protease inhibitor cocktail (Roche Diagnostics Ltd., Mannheim, Germany) (pH 7.2) and centrifuged at 21,000 \times g for 20 min at 4°C. The supernatant containing the extracellular soluble A β fraction was collected and stored at -80°C until further use. The A β ₄₂ concentrations in these samples were quantified using an A β ₄₂ ELISA kit (Invitrogen, Carlsbad, CA, USA) according to the manufacturer's instructions. The A β ₄₂ concentrations were normalised to total protein concentrations in the samples, determined with a BCA protein assay kit (Thermo Fischer Scientific, Waltham, MA, USA).

2.12 | Triglyceride and neutral lipid quantification

The lipid extraction from homogenised liver samples was performed as described by Bligh and Dyer ([1959](#)). The triglyceride concentrations in these lipid extractions and the serum were determined with an enzymatic reagent kit (DiaSys Diagnostic Systems, Holzheim, Germany), according to the manufacturer's instructions.

Hepatic neutral lipids were quantified in the liver sections, as described previously (Martens et al., [2021](#)). Tissue Tek-embedded samples of the left liver lobe were cut with a cryostat CM3050S (Leica, Wetzlar, Germany) to obtain 12- μ m sections which were mounted on SuperFrost Plus adhesion slides (Thermo Fisher Scientific, Waltham, USA) and stored at -20°C until use. The liver sections were fixed in 4% neutral buffered formalin, washed with tap water and

rinsed with 60% isopropanol. The hepatic neutral lipids were stained by incubating the sections with Oil Red O (Polysciences Inc., Warrington, USA) for 15 min. The liver sections were rinsed with 60% isopropanol and covered with a coverslip. Digital images of the sections were obtained with a Leica DMLB microscope (Leica Microsystems, Rijswijk, The Netherlands) equipped with software from the Leica Applications Suite (Leica Microsystems, Rijswijk, The Netherlands). The surface area of the Oil Red O staining was quantified using Fiji ImageJ software.

2.13 | Lipoprotein profile in serum

The cholesterol concentrations in very-low-density lipoproteins (VLDL), low-density lipoproteins (LDL) and high-density lipoproteins (HDL) in serum were determined using fast protein liquid chromatography (FPLC), as previously described (Fedoseienko et al., [2018](#); Larsen et al., [2022](#)). The system comprised a PU4180LPG quaternary pump with an LG-980-02 linear degasser, FP920 fluorescence and UV4075 UV/VIS detectors (Jasco, Tokyo, Japan). After injection of 25 μ l of serum (1:1 diluted in TBS [pH 7.4]), lipoproteins were separated using a Superose 6 HR 10/30 column (GE Healthcare Hoevelaken, The Netherlands), operating at a flow rate of 0.31 ml min⁻¹. An additional R-PU-4081i right extension pump (Jasco, Tokyo, Japan) was employed for introducing cholesterol PAP enzymatic reagent (Diasys, Holzheim, Germany) at a flow rate of 0.1 ml min⁻¹, facilitating cholesterol detection. Chromatogram analysis was conducted using ChromNav chromatographic software, version 2.0 (Jasco, Tokyo, Japan). For quantitative analysis of the separated lipoproteins, commercially available lipid plasma standards (low, medium and high) (SKZL, Nijmegen, The Netherlands) were employed.

2.14 | Statistical analyses

Statistical analyses were conducted with PRISM GraphPad 8, only for sample sizes of at least ≥ 5 . The presented group sizes, on which the statistical analyses were conducted, represent the number of independent values (i.e. excluding technical replicates as independent values). The data were analytically tested for normal distribution with the Shapiro-Wilk normality test and visually checked by plotting the data in a histogram. For data showing a normal distribution, we performed a two-way analysis of variance (ANOVA) with treatment and genotype as independent variables (if $P < 0.05$: post hoc test: Sidak). Not normally distributed data were analysed with a Mann-Whitney test, a Kruskal-Wallis test (if $P < 0.05$: post hoc: Dunn's), or the data went through a rank transformation followed by a two-way ANOVA with treatment and genotype as independent variables (if $P < 0.05$: post-hoc: Sidak). Significant differences ($\alpha = 0.05$) are indicated with an asterisk (*). Only for the behavioural data, extreme values, as determined by Dixon's exclusion principles (Dixon, [1950](#), [1951](#)), were excluded from further analysis.

The manuscript complies with the *BJP*'s recommendations and requirements on the experimental design and analysis (Curtis et al., 2022).

2.15 | Materials

22-Ketositosterol (IUPAC: 22-ketostigmast-5-en-3 β -ol; purity: 100%) was in-house synthesised (Maura Marinozzi's lab) starting from stigmast-5-en-3 β -ol *i*-methyl ether. Briefly, the latter was submitted to hydroboration/oxidation reaction to obtain a mixture of the four C-22/C23 hydroxylated derivatives, which was directly oxidised by Dess–Martin reagent, thus furnishing the inseparable mixture of 22- and 23-keto derivatives. The chromatographic separation of the two regioisomers was made possible after the conversion of the mixture into the corresponding 3 β -acetylated derivatives. Final hydrolysis of 3 β -acetoxy-22-ketostigmast-5-en-3 β -ol furnished 22-ketositosterol in 32% overall yield.

DMEM/F-12 medium, FCS, penicillin, streptomycin, gentamycin, L-glutamine, sodium pyruvate (Na-Pir), glucose and non-essential amino acids solution (NEAA) were purchased from Thermo Fisher Scientific (Waltham, MA, USA), while phorbol 12-myristate 13-acetate (PMA), Sandoz 58-035, bovine serum albumin (BSA), lipid-free human apolipoprotein A-I (ApoA-I) and human high-density lipoprotein (HDL) were purchased from Sigma-Aldrich (St. Louis, MO, USA). RPMI 1640 medium was obtained from Euroclone (Milan, Italy), and T091317 (#293754-55-9) was obtained from Cayman (Ann Arbor, MI, USA). Xylene and n-decane were from Roth (Karlsruhe, Germany). Buffered saline, 2-mercapto-ethanol, pyridine, hexamethyldisilazane, epicoprostanol, and 5- α -cholestane were obtained from Thermo Fisher Scientific. Cyclohexane, trimethylchlorosilane, Triton-X100, paraffin wax and 10% formalin were from Sigma-Aldrich.

Details of other materials and suppliers are provided in the specific sections

2.16 | Nomenclature of targets and ligands

Key protein targets and ligands in this article are hyperlinked to corresponding entries in the IUPHAR/BPS Guide to PHARMACOLOGY <http://www.guidetopharmacology.org> and are permanently archived in the Concise Guide to PHARMACOLOGY 2023/24 (Alexander et al., 2023).

3 | RESULTS

3.1 | Cell-type specific activation of LXR α and LXR β and up-regulation of LXR target genes

The results of the *in vitro* dual luciferase reporter assay demonstrated that 22-ketositosterol activates LXR α and LXR β in a cell-type-specific manner (Figure 1). LXR α and LXR β were comparably activated in

HEK293, SH-SY5Y and CHME3 cells. In CCF-STTG1 cells, 22-ketositosterol activated LXR β slightly more than LXR α (Figure 1).

As the promotion of cholesterol efflux in astrocytes is crucial for neuronal cholesterol supply, we assessed the effect of 22-ketositosterol on the expression of LXR-responsive cholesterol efflux genes in CCF-STTG1 cells and human astrocytes. The exploratory data suggest that 22-ketositosterol increases the expression of the LXR target genes *ABCA1*, *ABCG1* and *APOE*, which are involved in cholesterol efflux, in both cell types (Figure 2). 22-Ketositosterol demonstrated no effect on the expression caveolin 1 gene (*CAV1*), *SREBP1* or *SREBP2* in primary human astrocytes (data not shown).

3.2 | Cholesterol efflux is enhanced by 22-ketositosterol

The exploratory data suggest that 22-ketositosterol enhances the efflux of cholesterol from HepG2 cells to ApoA-I, HDL and human serum in a concentration-dependent manner (Figure 3a–c). In THP-1 cells, 22-ketositosterol may promote the efflux of cholesterol to ApoA-I (Figure 3d). However, the cholesterol efflux from THP-1 cells to HDL or human serum was only minimally affected (Figure 3e,f).

3.3 | 22-Ketositosterol is internalised by cells and affects cholesterol synthesis

Cellular internalisation of 22-ketositosterol was determined for the lowest concentration that activates LXRs *in vitro* (1.25 μ M). We demonstrated internalisation of 22-ketositosterol by CCF-STTG1, SH-SY5Y and HepG2 cells (Figure 4a). To examine the effect of 22-ketositosterol on cholesterol synthesis in these cell lines, we determined the concentrations of cholesterol and cholesterol precursors (Figure 4b). In line with the data demonstrating an enhanced cholesterol efflux (Figure 3), 22-ketositosterol reduced the intracellular concentrations of cholesterol and the cholesterol precursors, lanosterol, desmosterol and lathosterol in CCF-STTG1 cells. In HepG2 cells, 22-ketositosterol also reduced the concentrations of cholesterol, lanosterol and lathosterol, while the desmosterol concentration remained unaffected (Figure 4b). The concentrations of cholesterol and cholesterol precursors in SH-SY5Y cells were only minimally affected by 22-ketositosterol (Figure 4b).

As a proxy of cholesterol synthesis rate, the ratios of cholesterol precursors to cholesterol were determined (Figure 4c). We found that in CCF-STTG1 cells 22-ketositosterol increased lanosterol/cholesterol. 22-Ketositosterol also increased the ratios of desmosterol/cholesterol and lathosterol/desmosterol, but it did not reach statistical significance (Figure 4c). In SH-SY5Y and HepG2 cells, 22-ketositosterol also increased desmosterol/cholesterol (Figure 4c). The ratio of lathosterol/cholesterol was also increased; however, it did not reach statistical significance (Figure 4c). These data are indicative of an increased cholesterol synthesis.

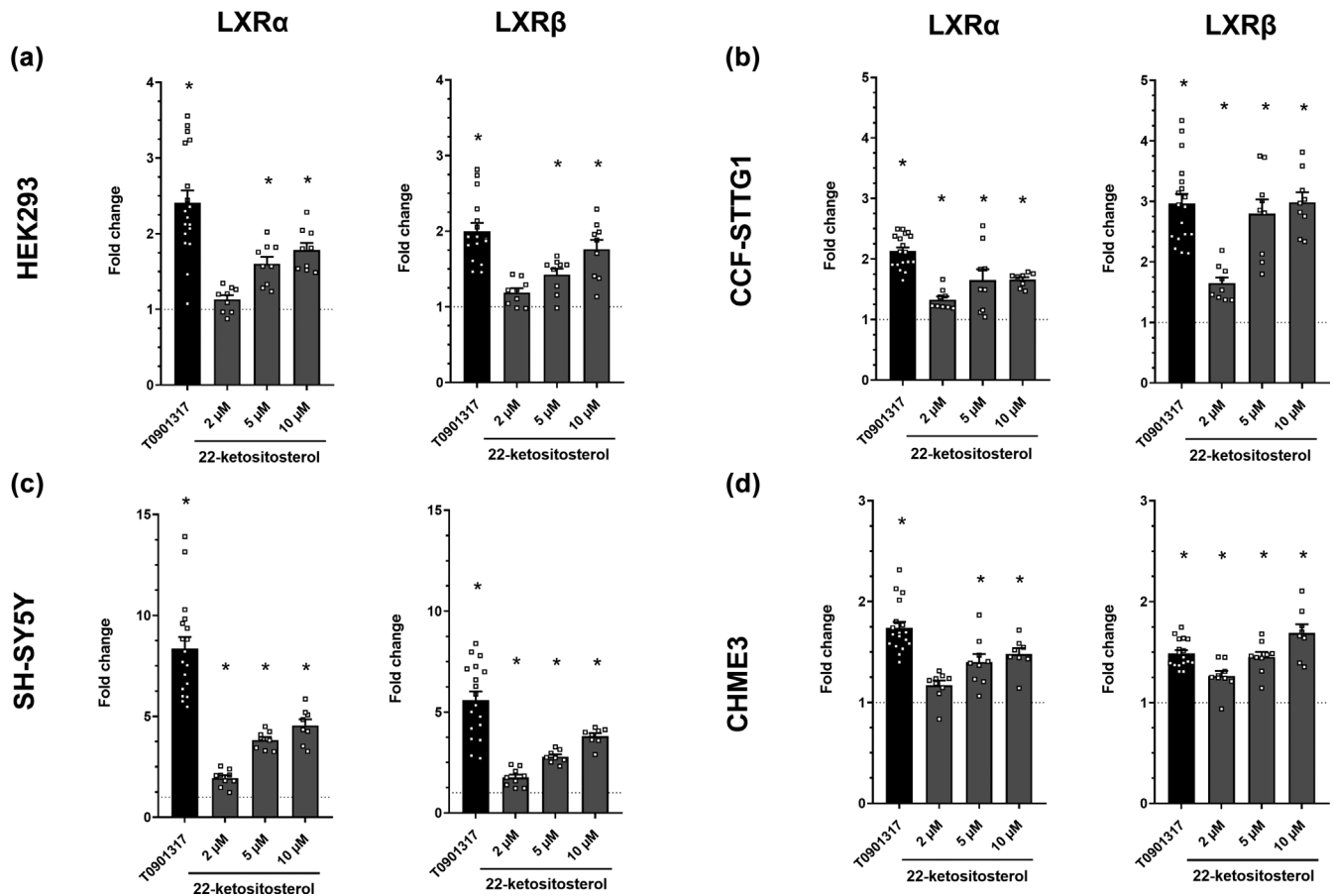


FIGURE 1 22-Ketositosterol activates LXR α and LXR β . 22-Ketositosterol was tested for its LXR α - and LXR β -activating ability in (a) HEK293, (b) CCF-STTG1, (c) SH-SY5Y and (d) CHME3 cells. The data are expressed as fold change of LXR α / β activation in cells incubated with LXR α / β agonist T0901317 or 22-ketositosterol (2, 5 or 10 μ M) relative to the activation in EtOH-incubated cells. Bars represent the mean \pm SEM ($n = 9$ [22-ketositosterol] or $n = 18$ [T0901317]). Data were analysed with a one-way ANOVA (Kruskal–Wallis test). Values relative to 1.0: * $P \leq 0.05$.

3.4 | 22-Ketositosterol was detectable in the cerebellum, liver, and circulation upon supplementation in mice

The analyses of the animal tissues revealed the presence of 22-ketositosterol in the cerebellum, liver, and serum of WT and APPswePS1 Δ E9 mice upon its supplementation to the diet. In APPswePS1 Δ E9 mice compared to WT mice, the concentration of 22-ketositosterol in the serum was higher, whereas the concentration found in the cerebellum of APPswePS1 Δ E9 mice was lower. 22-Ketositosterol was absent in the tissues of mice that received a non-supplemented, vehicle diet (Figure S2a–c).

3.5 | Effects of 22-ketositosterol on cognitive performance

At baseline, we confirmed a functional object location memory of both WT and APPswePS1 Δ E9 mice (Figure S1). Consistent with previous reports (Bogie et al., 2019; Martens et al., 2021), at the end of the 12-week treatment period, at the age of approximately 8.5 months,

non-supplemented APPswePS1 Δ E9 mice demonstrated cognitive deterioration (Figure 5a–c). Diet supplementation with 22-ketositosterol prevented the decline in the performance of APPswePS1 Δ E9 mice in the object location task (OLT; Figure 5a). However, the decline in the performance of these mice in the object recognition task (ORT; Figure 5b) and the Y-maze (Figure 5c) could not be prevented by 22-ketositosterol administration. 22-ketositosterol did not affect normal cognitive performance in WT mice in any of the tasks performed (Figure 5a–c).

3.6 | No effect of 22-ketositosterol on A β plaque load

Administration of 22-ketositosterol did not affect A β plaque load in the cortex nor in the hippocampus of the APPswePS1 Δ E9 mice (Figure 6a,b,e). The A β plaque load in the hippocampus subfields cornu ammonis 1 (CA1), cornu ammonis 2/3 (CA2/3) and dentate gyrus (DG) did not show an effect of 22-ketositosterol (Figure 6b). The immunohistochemical staining of A β aggregates revealed that most plaques were small sized (< 200 nm²), with no effect of

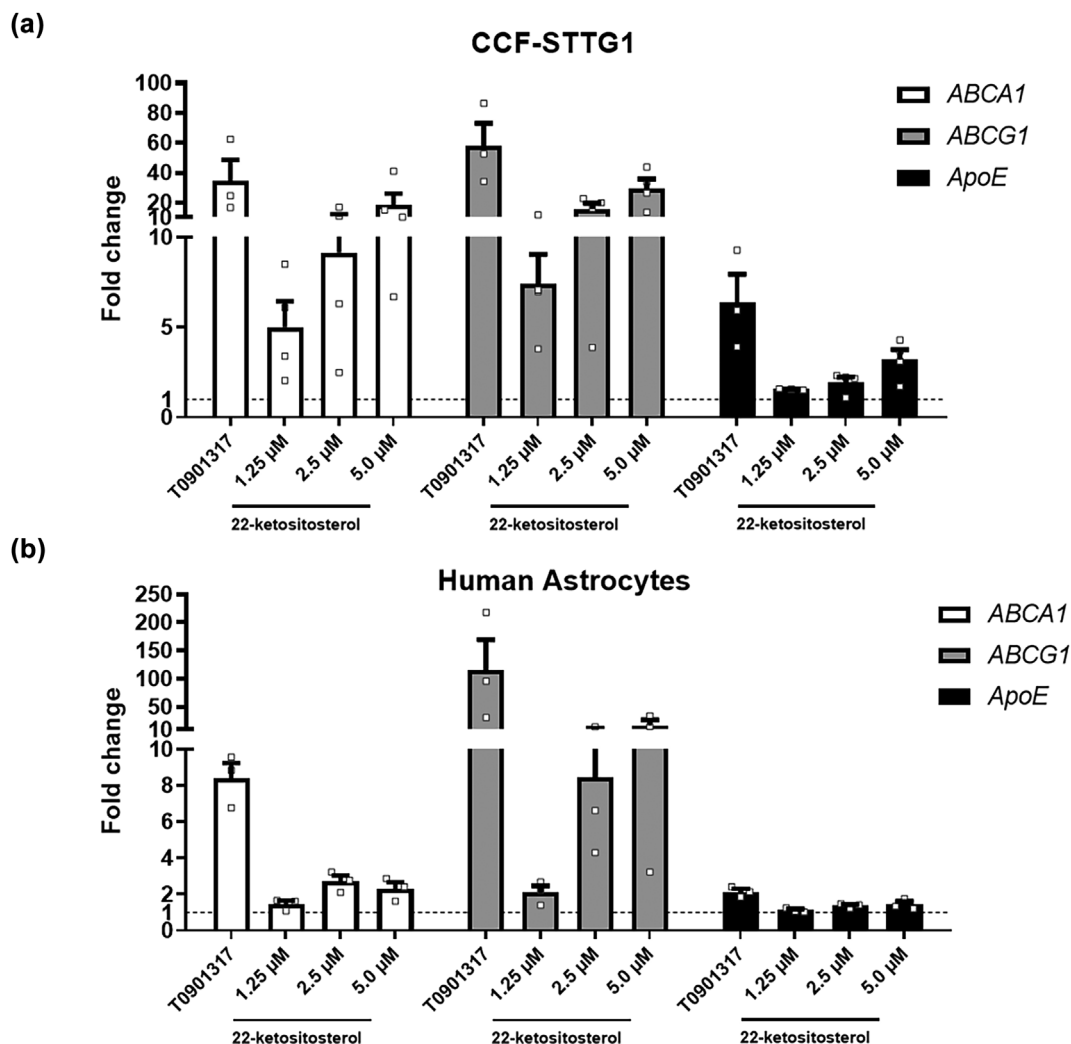


FIGURE 2 22-Ketositosterol increases the RNA expression of LXR-response genes involved in cholesterol efflux in (a) CCF-STTG1 cells and (b) primary human astrocytes. Gene expression of *ABCA1*, *ABCG1* and *APOE* was determined in CCF-STTG1 cells and human astrocytes incubated with 22-ketositosterol (1.25–5.0 μ M), T0901317 (2.5 μ M [CCF-STTG1] and 1 μ M [human astrocytes; HÅ]) as a positive control, or EtOH. Gene expression was normalised to the geometric mean of housekeeping genes *ACTB*, *B2M*, *HPRT1* and *SDHA* (CCF-STTG1) and, additionally, *YWHAZ* and *TBP* (human astrocytes), and expressed as fold change compared to the expression in EtOH-incubated cells. Bars represent the mean \pm SEM ($n = 3$ [human astrocytes] or 4 [CCF-STTG1 cells] from independent experiments).

22-ketositosterol on plaque size distribution (Figure 6c–e). The cortical soluble $A\beta_{42}$ concentrations also remained unaffected by 22-ketositosterol (Figure 6f).

3.7 | 22-Ketositosterol reduced the microglia markers ionized calcium-binding adaptor molecule 1 (*Iba1*) and CD68 in the brain

The microglia markers *Iba1* and CD68 were assessed by quantifying the relative surface area (%) after immunohistochemical staining of brain slices of WT and APPswePS1 Δ E9 mice (Figure 7). Independent of genotype, diet supplementation with 22-ketositosterol reduced the *Iba1* expression in the cortex (Figure 7a,c) and in the hippocampus (Figure 7b,c). 22-Ketositosterol decreased the *Iba1* expression in the

hippocampus of APPswePS1 Δ E9 mice but not in WT mice (Figure 7b). Analysis of the hippocampal areas cornu ammonis 1 (CA1), cornu ammonis 2/3 (CA2/3) and dentate gyrus (DG) separately provided similar results, with a genotype-independent decrease in *Iba1* (Figure 7b) and a significant decrease in *Iba1* expression in the hippocampus of APPswePS1 Δ E9 mice but not in WT mice (Figure 7b).

The expression of CD68, a marker that is abundantly expressed by phagocytes including microglia and macrophages and up-regulated with inflammation (Chistiakov et al., 2017), was significantly elevated in the cortex and, although not significantly, in the hippocampus of APPswePS1 Δ E9 mice as compared to WT mice (Figure 7d–f). 22-Ketositosterol supplementation resulted in a genotype-independent decrease in CD68 expression in the cortex (Figure 7d). 22-Ketositosterol decreased the CD68 expression in the cortex of

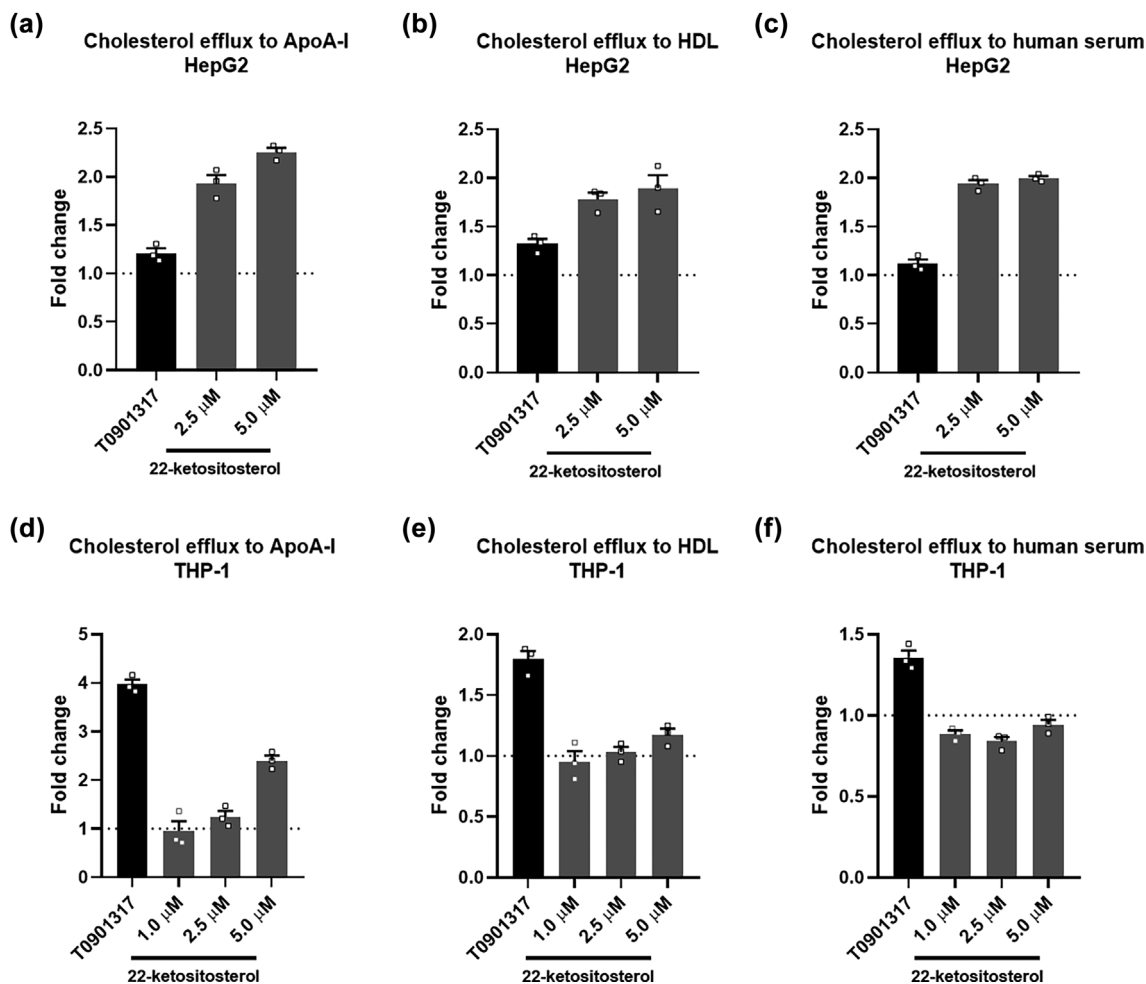


FIGURE 3 Effect of 22-ketositosterol on cholesterol efflux in HepG2 and THP-1 cells. Cholesterol efflux from (a–c) HepG2 and (d–f) THP-1 cells to ApoA-I ($10 \mu\text{g ml}^{-1}$) (Figure 3a,d), HDL ($12.5 \mu\text{g ml}^{-1}$) (Figure 3b,e) and human serum (2%) (Figure 3c,f) was determined after incubation with 22-ketositosterol (1.0, 2.5 or 5.0 μM) or T0901317 (1 μM) as a positive control. The data are expressed as cholesterol efflux relative to the efflux in EtOH-incubated cells. Bars represent the mean \pm SEM ($n = 9$).

APPswePS1 Δ E9 mice but did not reach statistical significance (Figure 7d). The CD68 expression in the hippocampus was also reduced upon 22-ketositosterol administration, but no statistical significance was reached (Figure 7e).

3.8 | The elevated GFAP expression in the cortex of APPswePS1 Δ E9 mice was decreased by 22-ketositosterol

The GFAP expression in the cortex of APPswePS1 Δ E9 mice was elevated compared to WT mice, as determined by the relative surface area (%) of immunohistochemical staining (Figure 8). Independent of genotype, 22-ketositosterol supplementation was demonstrated to decrease the GFAP expression in the cortex. 22-Ketositosterol decreased the GFAP expression in the cortex of APPswePS1 Δ E9 mice but not in the cortex of WT mice (Figure 8a,c). The GFAP expression in the hippocampus of APPswePS1 Δ E9 mice did not differ from that in WT mice and was not affected by 22-ketositosterol supplementation (Figure 8b,c).

3.9 | 22-Ketositosterol supplementation affected the sterol profiles

The concentrations of cholesterol (Figure 9), and its precursors (lanosterol, desmosterol and lathosterol) and metabolites (24-hydroxycholesterol [24-OHC], 27-hydroxycholesterol [27-OHC], 7 α -hydroxycholesterol [7 α -OHC] and cholestanol) (Figure S3) were determined in the cerebellum, liver and serum. As a proxy of the cholesterol synthesis and oxidation, we determined the ratios of cholesterol precursors and metabolites to cholesterol, respectively (Table 2).

The cholesterol concentration in the liver of APPswePS1 Δ E9 mice was significantly higher compared to WT mice, while no significant differences were observed in serum and cerebellum cholesterol levels. In contrast, the concentration of the cholesterol precursor lanosterol, along with its ratio to cholesterol, was significantly lower in the cerebellum of APPswePS1 Δ E9 mice compared to WT mice. The lanosterol concentration in the liver and the lanosterol-to-cholesterol ratio in the serum were elevated in APPswePS1 Δ E9 mice. Additionally, the desmosterol concentration in the liver and the desmosterol-

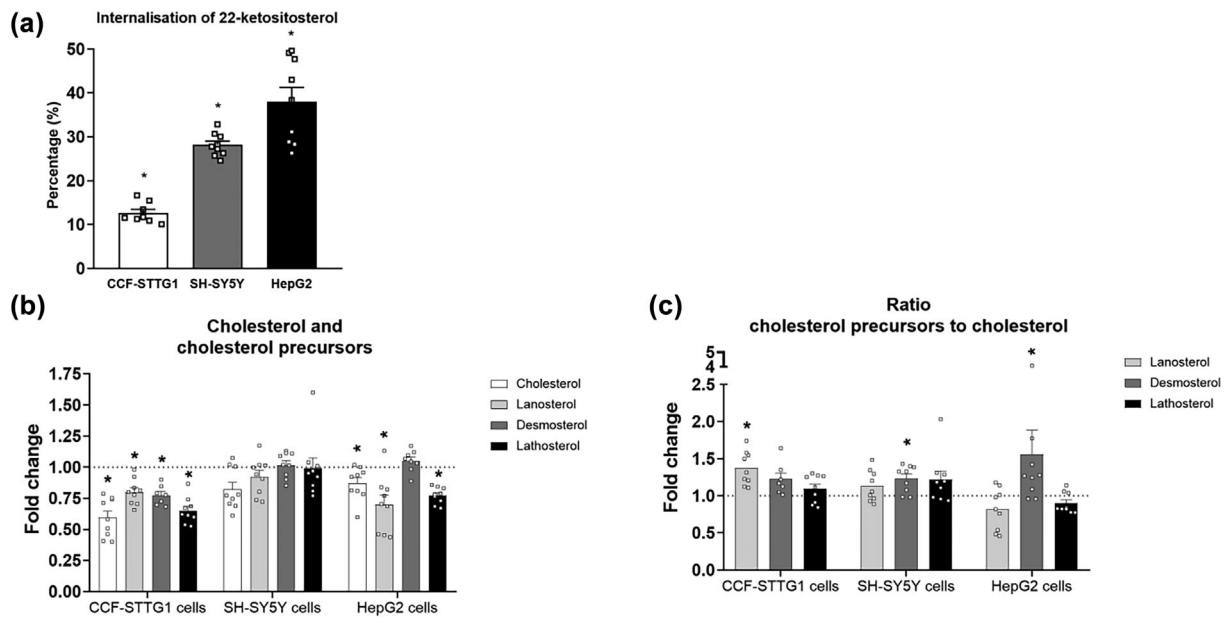


FIGURE 4 The effects of 22-ketotestosterone on cholesterol and cholesterol precursors. (a) Cellular internalisation of 22-ketotestosterone was determined in CCF-STTG1, SH-SY5Y and HepG2 cells incubated with 22-ketotestosterone (1.25 μ M) for 24 h. (b) The concentrations of cholesterol and cholesterol precursors lanosterol, desmosterol, and lathosterol were determined in these cells after 24-h incubation with 22-ketotestosterone (1.25 μ M) and expressed as fold change relative to EtOH-incubated cells. (c) The ratios of cholesterol precursors to cholesterol are also expressed as fold change relative to EtOH-incubated cells. The bars represent the mean \pm SEM ($n = 9$). Data were analysed with a one-sample t -test to test for significance to 0% (Figure 4a) or a Mann-Whitney test to test for significance to EtOH-incubated cells (Figure 4b,c). * $P \leq 0.05$.

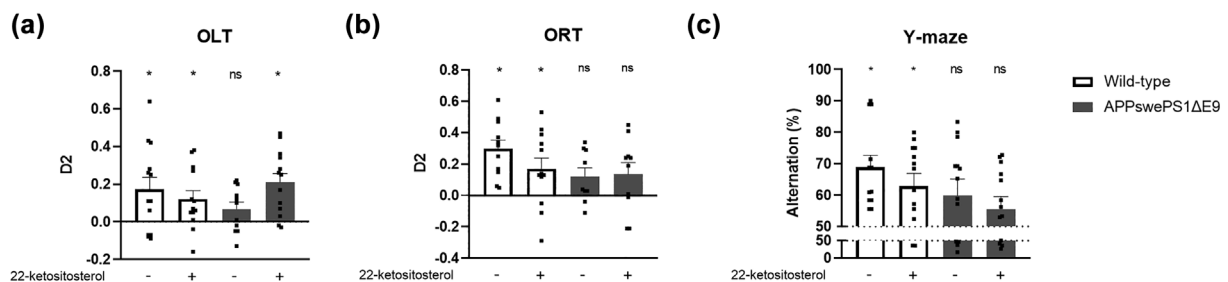


FIGURE 5 Diet supplementation with 22-ketotestosterone prevents spatial memory loss but not recognition memory or spatial working memory loss in APPswePS1 Δ E9 mice. The effect of diet supplementation of 22-ketotestosterone on cognitive performance was determined using an (a) object location task (OLT), (b) an object recognition task (ORT), and (c) a spontaneous alternation Y-maze test. Extreme values (OLT: APPswePS1 Δ E9-vehicle $n = 1$; ORT: APPswePS1 Δ E9-vehicle $n = 1$), as determined by Dixon's exclusion principles, have been excluded from the analyses. Bars represent the mean \pm SEM ($n = 9$ –13 per group). Data were analysed with a one-sample t -test compared to 0. D2 values relative to 0: * $P \leq 0.05$, ns: no significant difference detected.

to-cholesterol ratio were elevated in APPswePS1 Δ E9 mice compared to WT mice.

In the cerebellum, APPswePS1 Δ E9 mice showed significantly higher concentrations of the cholesterol metabolite 7 α -OHC and its ratio to cholesterol, while the cholestanol concentration and its ratio to cholesterol were lower compared to WT mice. In the liver, the concentrations of cholesterol metabolites 24-OHC, 27-OHC and 7 α -OHC were elevated in APPswePS1 Δ E9 mice, along with the ratios of 24-OHC and 7 α -OHC to cholesterol. In the serum, elevated ratios of 24-OHC, 7 α -OHC and cholestanol to cholesterol were observed in APPswePS1 Δ E9 as compared to the WT mice.

The cholesterol concentrations in the cerebellum remained unaffected by 22-ketotestosterone (Figure 9a). However, 22-ketotestosterone did affect the concentrations of cholesterol precursors and metabolites (Figure S3 and Table 2). In the cerebellum of WT mice but not in APPswePS1 Δ E9 mice, 22-ketotestosterone administration decreased the ratios of lanosterol/cholesterol, desmosterol/cholesterol and lathosterol/cholesterol in the cerebellum, indicating a reduced cholesterol synthesis (Table 2). Regarding cholesterol metabolites in the cerebellum, 22-ketotestosterone administration increased 7 α -OHC/cholesterol independent of genotype but demonstrated no significant increase in either APPswePS1 Δ E9 or

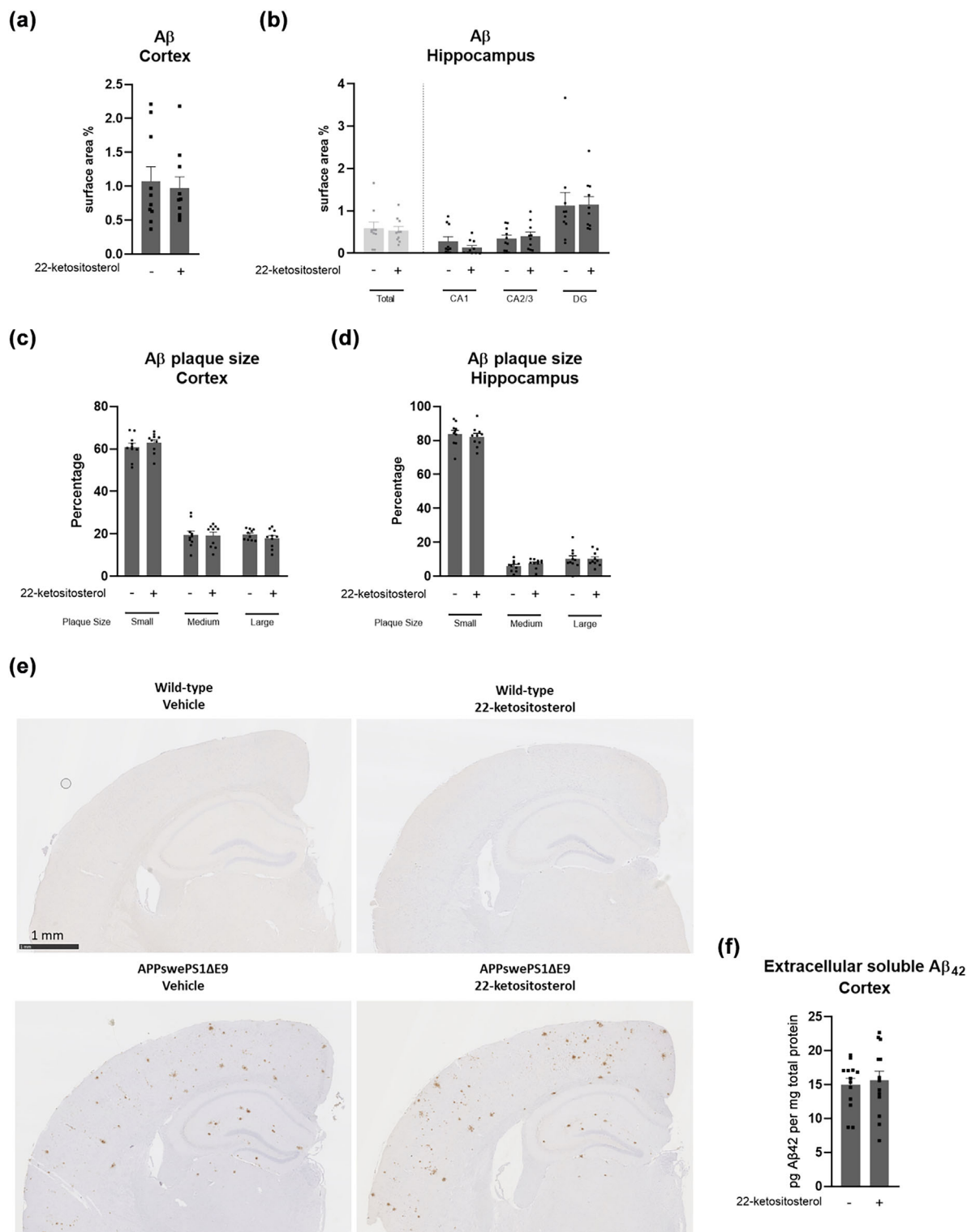


FIGURE 6 No effect of 22-ketotestosterone on Aβ plaque load in APPswePS1ΔE9 mice. After immunohistochemical staining of brain slices with Aβ, the Aβ plaque load in the (a) cortex and (b) hippocampus was determined as the surface area percentage of the staining ($n = 10$ per group, one slice per animal). The percentage of small ($< 200 \mu\text{m}^2$), medium ($200\text{--}450 \mu\text{m}^2$) and large ($> 450 \mu\text{m}^2$) plaques were calculated in the (c) cortex and (d) hippocampus. Representative images of the Aβ staining are presented in Figure 6e. (f) Extracellular soluble Aβ₄₂ was measured in the cortex with an ELISA ($n = 13$ per group). Bars represent the mean \pm SEM. Data presented in Figure 6a,b were analysed with a Mann-Whitney U test. Data presented in Figure 6c–e were analysed with an unpaired t -test. None of the differences between vehicle-treated and 22-ketotestosterone-treated mice were statistically significant.

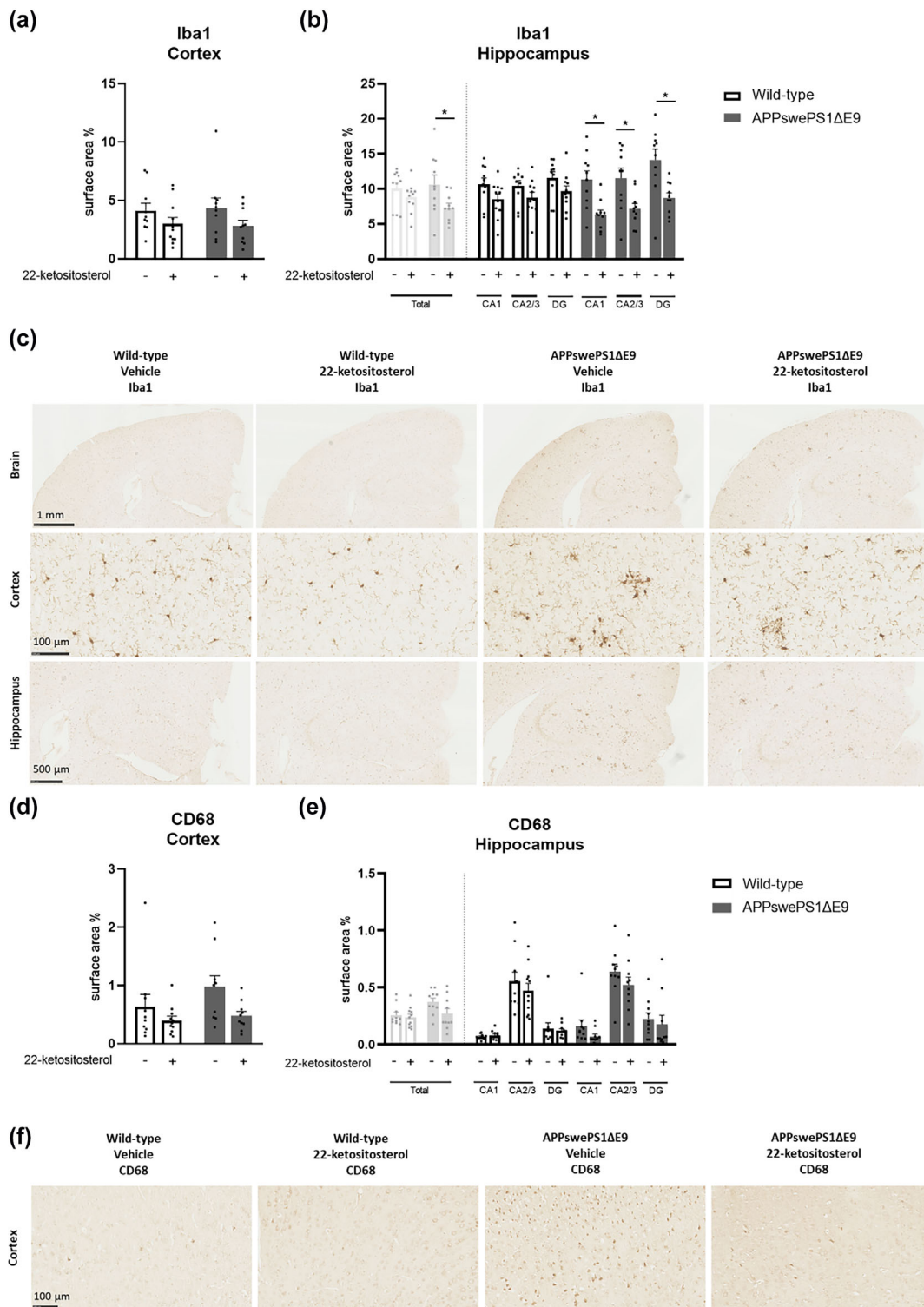


FIGURE 7 22-Ketotestosterone reduces microglia markers Iba1 and CD68 in the cortex and the hippocampus. The cortical and hippocampal surface area percentages of (a–c) Iba1 and (d–f) CD68 staining were determined after immunohistochemical staining of brain slices of WT and APPswePS1ΔE9 mice ($n = 10–11$ per group, three cortical images and one hippocampus image of one slice per animal). Representative images of the Iba1 and CD68 staining are presented in Figure 7c,f, respectively. Bars represent the mean \pm SEM. All data in this figure were analysed with a two-way ANOVA with a Sidak post hoc test, prior to which data presented in Figure 7b,d,e went through a rank transformation. * $P \leq 0.05$.

WT mice. 22-Ketotestosterone decreased the cholestanol/cholesterol ratio only in the cerebellum of APPswePS1ΔE9 mice and not in WT mice (Table 2).

In the liver, 22-ketotestosterone administration decreased the cholesterol concentration in both APPswePS1ΔE9 and WT mice (Figure 9b). 22-Ketotestosterone increased the ratio of desmosterol/

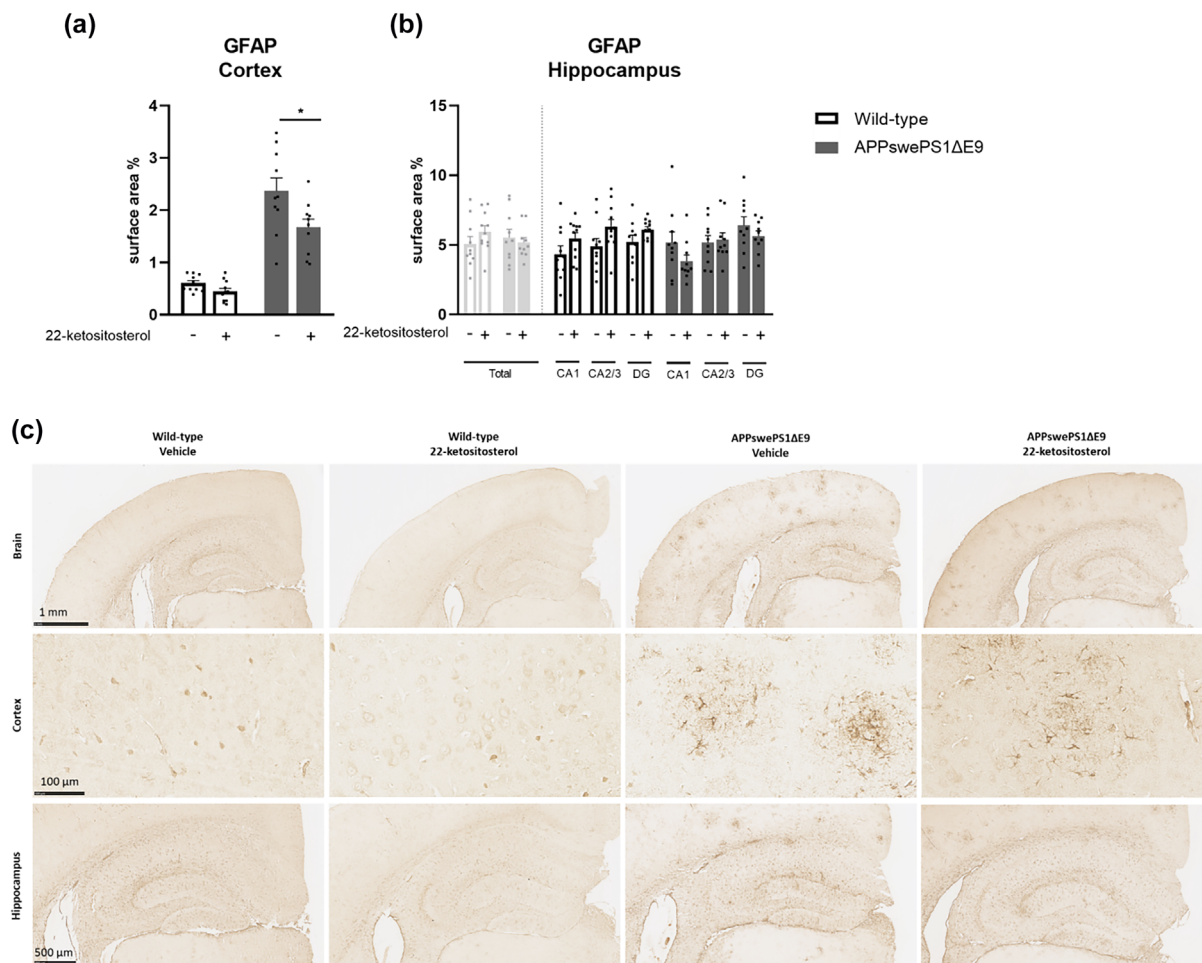


FIGURE 8 Diet supplementation with 22-ketositosterol prevents the increase in astrocyte marker GFAP in the cortex of APPswePS1ΔE9 mice. The surface area percentages of GFAP staining in the (a) cortex and (b) hippocampus of WT and APPswePS1ΔE9 mice are shown. Representative images of the GFAP staining are presented in Figure 8c. Bars represent the mean \pm SEM ($n = 10$ – 11 per group, three cortical images and one hippocampus image of one slice per animal). Data were analysed with a two-way ANOVA (post hoc: Sidak). * $P \leq 0.05$.

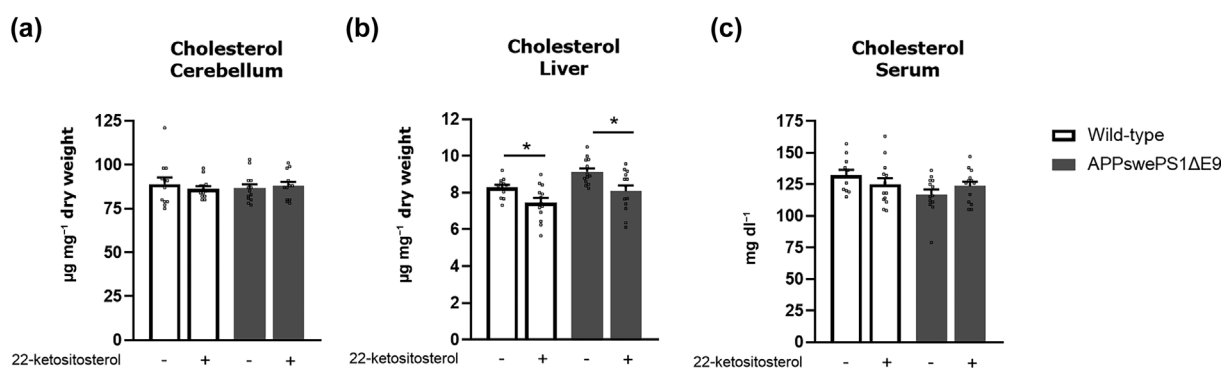


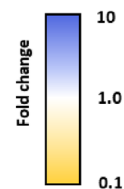
FIGURE 9 The concentrations of cholesterol in the (a) cerebellum, (b) liver and (c) serum of WT and APPswePS1ΔE9 mice after 22-ketositosterol supplementation. Bars represent the mean \pm SEM ($n = 12$ – 13 per group). Data were analysed with a two-way ANOVA (post hoc: Sidak). * $P \leq 0.05$.

cholesterol in APPswePS1ΔE9 mice but not in WT mice. 22-Ketositosterol supplementation increased the ratios of 24-OHC/cholesterol and 7 α -OHC/cholesterol and decreased cholestanol/cholesterol, but only in WT mice (Table 2).

Serum cholesterol concentrations were not affected by 22-ketositosterol (Figure 9c). However, the ratio of 27-OHC/cholesterol was decreased in both APPswePS1ΔE9 and WT mice. The ratio of cholestanol/cholesterol was decreased but only in WT mice (Table 2).

TABLE 2 Ratios of cholesterol precursors, cholesterol metabolites and campesterol to cholesterol concentrations.

	Cerebellum			
	Wild-type		APPswePS1ΔE9	
	Vehicle	22-ketositosterol	Vehicle	22-ketositosterol
Cholesterol precursors				
Lanosterol/cholesterol	1.00 ± 0.18	0.83 ± 0.06 *	0.75 ± 0.06	0.74 ± 0.10
Desmosterol/cholesterol	1.00 ± 0.15	0.86 ± 0.10 *	0.97 ± 0.13	0.92 ± 0.15
Lathosterol/cholesterol §	1.00 ± 0.21	0.80 ± 0.11 *	0.89 ± 0.14	0.86 ± 0.18
Cholesterol metabolites				
24-OHC/cholesterol §	1.00 ± 0.29	0.79 ± 0.24	0.79 ± 0.08	0.79 ± 0.10
27-OHC/cholesterol	1.00 ± 0.28	1.12 ± 0.17	1.08 ± 0.31	0.95 ± 0.24
7α-OHC/cholesterol	1.00 ± 0.38	1.28 ± 0.32	1.58 ± 0.26	1.85 ± 0.48
Cholestanol/cholesterol §	1.00 ± 0.26	1.04 ± 0.15	0.97 ± 0.47	0.51 ± 0.34 *
	Liver			
	Wild-type		APPswePS1ΔE9	
	Vehicle	22-ketositosterol	Vehicle	22-ketositosterol
Cholesterol precursors				
Lanosterol/cholesterol	1.00 ± 0.36	1.02 ± 0.41	0.99 ± 0.30	1.30 ± 0.48
Desmosterol/cholesterol §	1.00 ± 0.16	1.30 ± 0.65	1.18 ± 0.19	1.44 ± 0.26 *
Lathosterol/cholesterol	1.00 ± 0.21	0.98 ± 0.32	0.91 ± 0.17	1.07 ± 0.28
Cholesterol metabolites				
24-OHC/cholesterol §	1.00 ± 0.18	1.53 ± 0.44 *	2.05 ± 0.42	2.50 ± 0.81
27-OHC/cholesterol §	1.00 ± 0.23	1.01 ± 0.21	1.16 ± 0.21	1.06 ± 0.26
7α-OHC/cholesterol §	1.00 ± 0.33	2.36 ± 1.19 *	4.39 ± 1.64	6.27 ± 5.42
Cholestanol/cholesterol §	1.00 ± 0.14	0.86 ± 0.17 *	0.91 ± 0.12	0.87 ± 0.23
Campesterol/cholesterol	1.00 ± 0.18	0.84 ± 0.21	1.05 ± 0.19	0.91 ± 0.31
	Serum			
	Wild-type		APPswePS1ΔE9	
	Vehicle	22-ketositosterol	Vehicle	22-ketositosterol
Cholesterol precursors				
Lanosterol/cholesterol	1.00 ± 0.23	1.07 ± 0.27	1.13 ± 0.28	1.45 ± 0.51
Desmosterol/cholesterol §	1.00 ± 0.13	1.18 ± 0.51	1.09 ± 0.22	1.16 ± 0.24
Lathosterol/cholesterol	1.00 ± 0.21	0.98 ± 0.20	1.00 ± 0.19	1.16 ± 0.25
Cholesterol metabolites				
24-OHC/cholesterol §	1.00 ± 0.15	0.98 ± 0.08	1.14 ± 0.18	1.25 ± 0.57
27-OHC/cholesterol §	1.00 ± 0.12	0.76 ± 0.08 *	1.02 ± 0.12	0.83 ± 0.17 *
7α-OHC/cholesterol §	1.00 ± 0.32	0.96 ± 0.12	1.12 ± 0.28	1.04 ± 0.17
Cholestanol/cholesterol	1.00 ± 0.13	0.81 ± 0.11 *	1.10 ± 0.13	0.99 ± 0.21
Campesterol/cholesterol	1.00 ± 0.12	0.87 ± 0.13	1.22 ± 0.17	1.02 ± 0.31 *



Note: The data are relative to the ratios of vehicle-treated WT mice and presented as the mean ± SD ($n = 11-13$ per group). Data were analysed with two-way ANOVA (post-hoc: Sidak) prior to which the parameters indicated with § went through a rank transformation. Significance relative to vehicle-treated animals of the same genotype:

* $P \leq 0.05$.

3.10 | Modulatory effects of 22-ketositosterol on phytosterols

Diet supplementation with 22-ketositosterol lowered phytosterol concentrations in the cerebellum, liver and serum of APPswePS1ΔE9 and in WT mice (Figure 10a-c). 22-Ketositosterol reduced the campesterol/cholesterol ratio in the serum and liver (Table 2), which is indicative of a reduced intestinal sterol absorption.

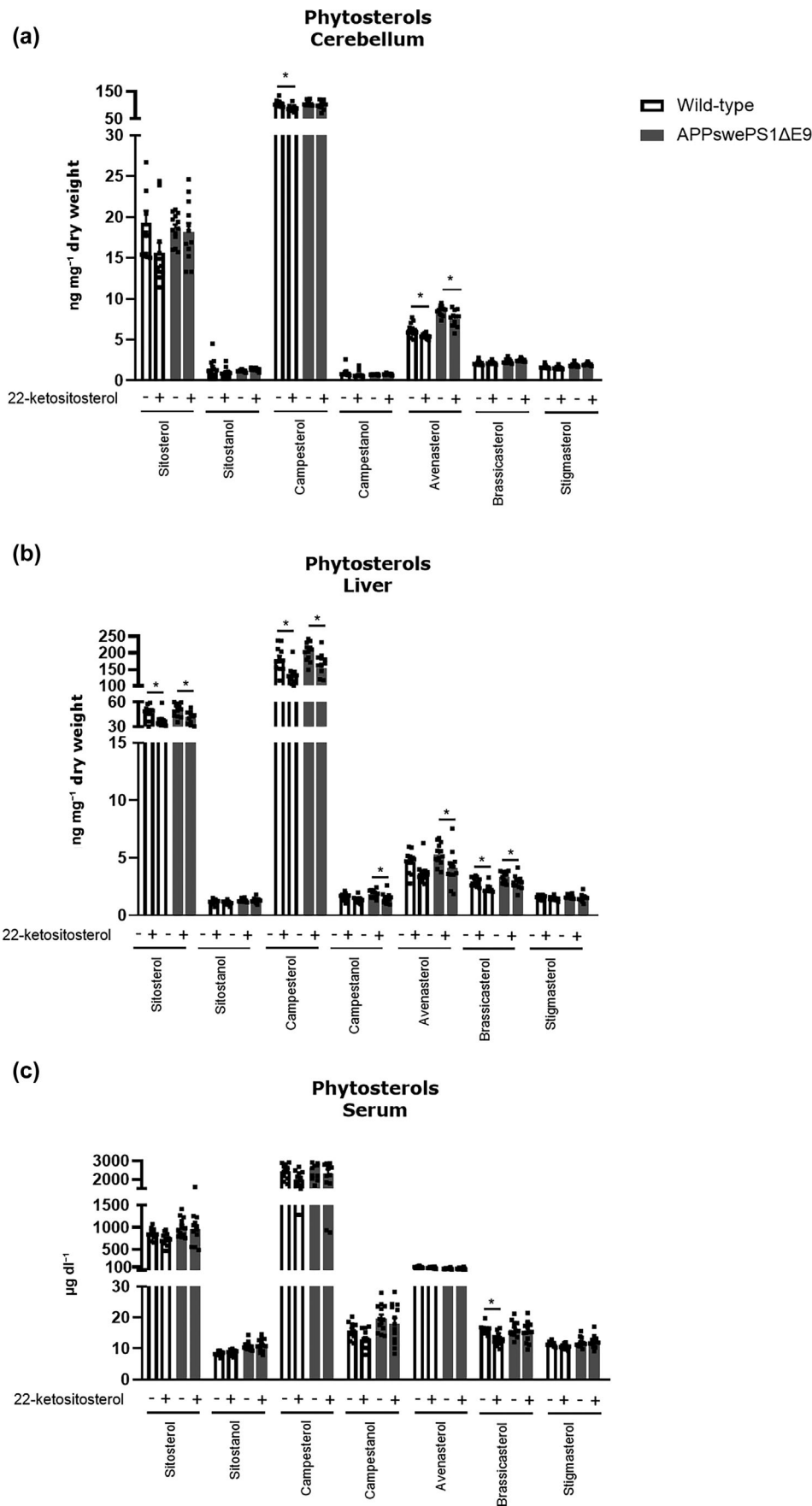
3.11 | No adverse effects of 22-ketositosterol on liver and serum triglyceride concentrations

To determine if 22-ketositosterol induces lipid accumulation in the liver and serum, as previously observed for synthetic LXRα/β

activators such as T0901317 (Grefhorst et al., 2002; Repa et al., 2000; Schultz et al., 2000), we quantified serum and hepatic triglycerides and hepatic neutral lipids. Moreover, we recorded the daily food intake and the body weight throughout the experiment. In line with our previous observations, APPswePS1ΔE9 mice gained more weight during the experiment than WT mice (Figure 11b,c), even though the food intake did not differ between APPswePS1ΔE9 and WT (Figure 11a). APPswePS1ΔE9 mice also showed elevated hepatic triglycerides (Figure 11e) and neutral lipids (Figure 11f).

The animals receiving a 22-ketositosterol-supplemented diet showed a higher food intake compared to vehicle-treated animals (Figure 11a). However, this was not reflected by differences in weight as 22-ketositosterol supplementation did not result in weight gain in the animals (Figure 11b,c). The administration of 22-ketositosterol did

FIGURE 10 Phytosterol concentrations in the (a) cerebellum, (b) liver and (c) serum of WT and APPswePS1ΔE9 mice after 22-ketositosterol supplementation. Bars represent the mean ± SEM (*n* = 12–13 per group). Data were analysed with a two-way ANOVA (post hoc: Sidak). * *P* ≤ 0.05.



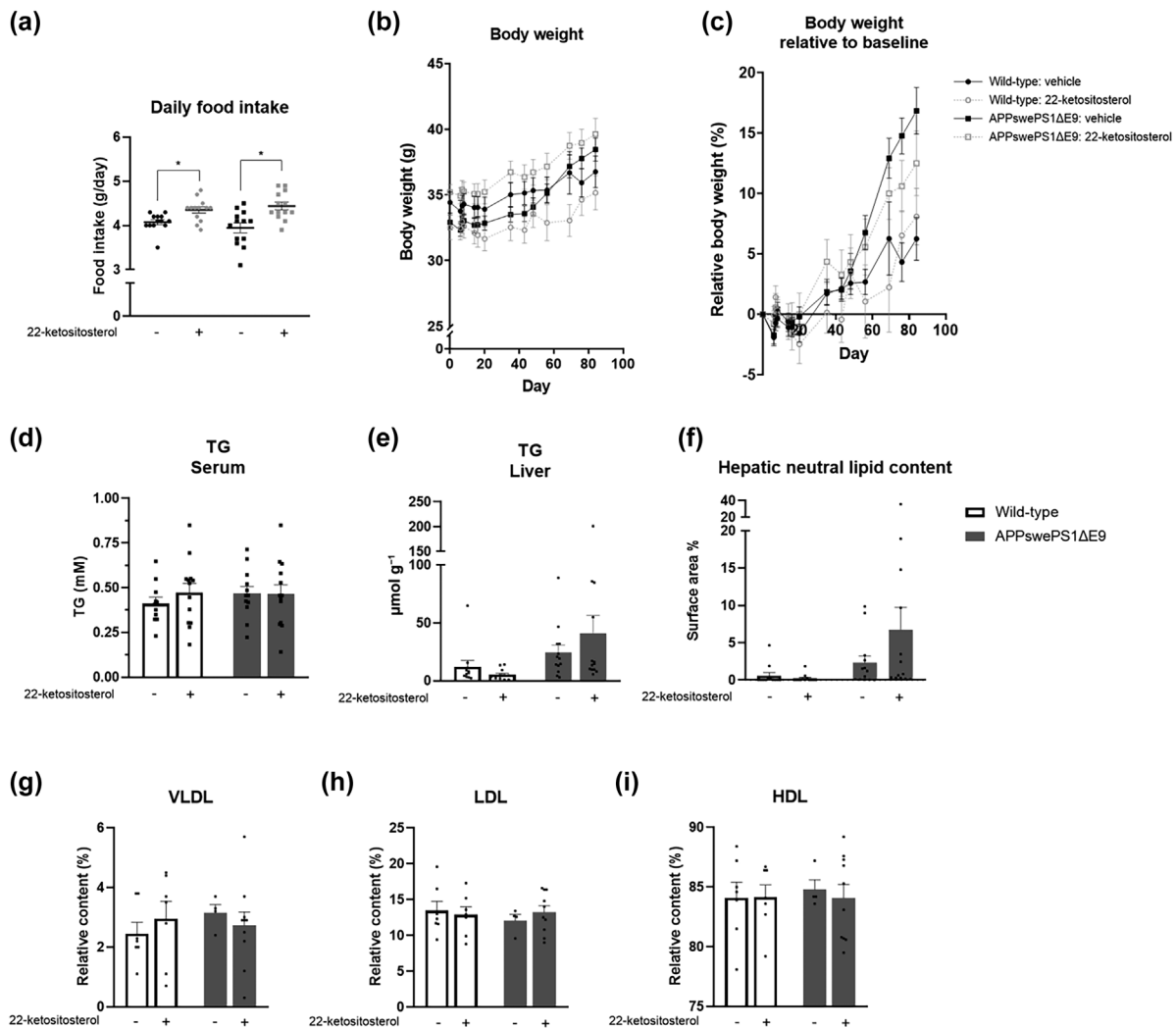


FIGURE 11 Food intake, body weight and lipid content of serum and liver after diet supplementation with 22-ketositosterol. The (a) daily food intake, (b) body weight, (c) body weight relative to baseline, (d, e) serum and liver triglyceride (TG) concentrations, and the (f) hepatic neutral lipid content determined by the surface area percentage of Oil Red O staining are presented ($n = 11-13$). The relative levels of (g) VLDL-c, (h) LDL-c and (i) HDL-c are presented ($n = 4-10$ per group). Data are presented as mean \pm SEM and analysed with two-way ANOVA (post hoc: Sidak), prior to which the data in Figure 11a,e,f went through a rank transformation. * $P \leq 0.05$.

not significantly affect serum triglyceride concentrations (Figure 11d) nor liver triglyceride concentrations (Figure 11e). Likewise, no effect was detected on the hepatic neutral lipid content (Figure 11f), nor on the relative levels of VLDL-c, LDL-c or HDL-c (Figure 11g-i).

The expression of *SREBF1* and its target genes *FASN* and *SCD1* in the liver remained unaffected by 22-ketositosterol supplementation (Figure 12a-c), whereas the *ACACA* expression was found to decrease, although it did not reach statistical significance in WT or APPswePS1ΔE9 mice (Figure 12c). 22-Ketositosterol supplementation did not significantly alter the expression of *G0/G1 Switch Gene 2* (*G0S2*) (Figure 12e), encoding a selective LXR α -responsive inhibitor of intracellular lipolysis of which an up-regulation is believed to contribute to the adverse effects of LXR α activation on lipid accumulation (Heckmann et al., 2017).

4 | DISCUSSION

We investigated the impact of the semi-synthetic LXR-activating oxysterol 22-ketositosterol on Alzheimer's disease (AD)-related pathology in APPswePS1ΔE9 mice. Our data demonstrate that 22-ketositosterol administered via the diet enters the brain and may prevent the decline in cognitive performance of APPswePS1ΔE9 mice. Administration of 22-ketositosterol did not influence A β plaque load, yet it notably reduced the expression of microglia and astrocyte inflammatory markers Iba1, CD68 and GFAP in the brain, suggesting anti-inflammatory effects. 22-Ketositosterol administration did not induce triglyceride accumulation in the liver or serum, unlike previously tested synthetic agonists such as T0901317 (Grefhorst et al., 2002; Repa et al., 2000; Schultz et al., 2000). *In vitro*, 22-ketositosterol was

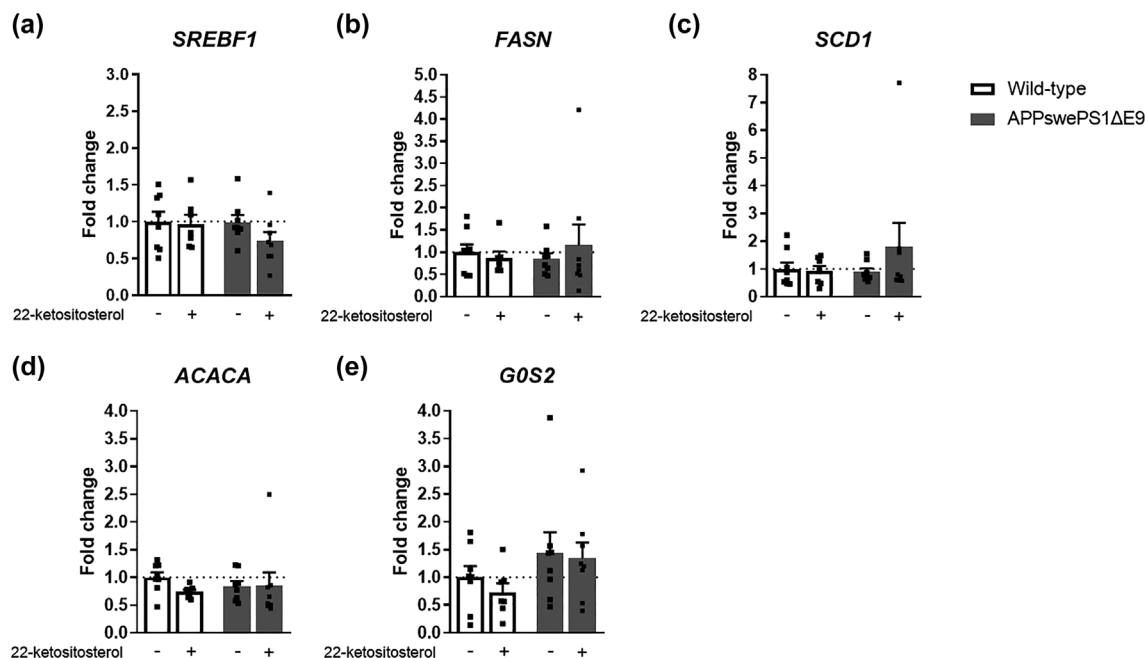


FIGURE 12 RNA expression of SREBF1, its target genes FASN, SCD1 and ACACA, and G0S2 in the liver after supplementation with 22-ketositosterol. The gene expression was normalised to the most stable housekeeping genes (ACTB, B2M, HPRT1 and SDHA) and expressed as fold change compared to the expression in vehicle-treated animals. Data are presented as mean \pm SEM ($n = 7-8$) and analysed with two-way ANOVA (post hoc: Sidak), prior to which the data in Figure 12b-e went through a rank transformation. None of the differences between vehicle-treated and 22-ketositosterol-treated mice were statistically significant.

found to activate LXR β slightly more than LXR α in CCF-STTG1 cells but comparably activated LXR α and LXR β in the other cell types tested. Besides, 22-ketositosterol was found to promote cholesterol efflux from cultured THP1 and HepG2 cells.

22-Ketositosterol demonstrated differential effects on the cognitive function of APPswePS1ΔE9 mice across the different tests. In line with 24(S)-saringosterol (Martens et al., 2021), 22-ketositosterol demonstrated a protective effect against the decline in hippocampus-dependent spatial memory, as evaluated by the OLT. However, unlike 24(S)-saringosterol (Martens et al., 2021), 22-ketositosterol did not prevent the decline in recognition memory and spatial working memory as evaluated with the ORT and Y-maze and involving both the hippocampus and cortical structures (Bai et al., 2012; Vogel-Ciernia & Wood, 2014). These data suggest that 22-ketositosterol may prevent a decline in hippocampus functions without significantly influencing cortical functions. However, each test has its sensitivity and therefore improvements may be more easily detected in one test over the other. Further investigation of various aspects of the cognitive function is necessary to validate the impact of 22-ketositosterol on cognitive performance.

Although 22-ketositosterol administration did not reduce the A β plaque load, it decreased the levels of inflammation-related microglia and astrocyte markers Iba1, CD68 and GFAP in the hippocampus and/or cortex of APPswePS1ΔE9 mice. This is in accordance with our previous findings upon 24(S)-saringosterol treatment in AD mice (Martens et al., 2021). These data suggest anti-inflammatory effects of 22-ketositosterol, which is supported by previous findings of

Marinozzi et al. demonstrating a decrease in LPS-induced TNF α expression by human monocytes (U937 cell line) with 22-ketositosterol (Marinozzi et al., 2017). Self-resolving inflammation is necessary for tissue regeneration after damage; however, uncontrolled and excessive inflammation can permanently damage neuronal tissue and play a significant role in the development and progression of AD (Heneka et al., 2015; Yong et al., 2019). Neuroinflammation is associated with the activation of microglia and astrocytes and the subsequent release of inflammatory cytokines and chemokines (Heneka et al., 2015). Compared to WT mice, APPswePS1ΔE9 mice displayed elevated levels of CD68 and GFAP cortex, signifying a potential excessive activation of microglia and astrocytes. The reduction of these CD68 and GFAP levels observed upon 22-ketositosterol treatment could indicate a reduction in glial activation and might partially mitigate the neuroinflammatory component of AD-related pathology. The disturbance of the surveilling and patrolling microglia in their housekeeping functions, including the removal of A β , can be negatively affected because of the activation of microglia. While reducing excessive glial activation might mitigate neuroinflammation, it is important to note that glial activation is crucial for normal brain functions like neuroprotection, synaptic regulation and maintenance of homeostasis. Thus, mitigating excessive glial activation may be beneficial, but it is important that 22-ketositosterol administration preserves normal glial activity to maintain these essential processes.

In line with the up-regulation of LXR target genes involved in cholesterol efflux (Marinozzi et al., 2017), our data suggest that 22-ketositosterol enhances cholesterol efflux in HepG2 and THP-1

cells. A promotion of cholesterol efflux may underlie the observed decrease in inflammation-related microglia and astrocyte markers in the brains of APPswePS1ΔE9 mice. By promoting cholesterol efflux, 22-ketositosterol may have the potential to ameliorate the cytotoxic accumulation of intracellular cholesterol that induces inflammasome activation (Westerterp et al., 2018). This is of particular interest when high amounts of cholesterol-rich cellular debris are released in neurodegenerative conditions, which are primarily cleared by microglia (Berghoff et al., 2021; Cantuti-Castelvetri et al., 2018). Additionally, activation of immune cells results in coordinated up-regulation of cholesterol synthesis and storage (Lee & Bensinger, 2022). Therefore, glial activation may be dampened by enhancing cholesterol efflux and reducing intracellular cholesterol. Enhancement of cholesterol efflux has been found to protect neuronal functioning and cognitive performance in mouse models of AD (Donkin et al., 2010; Jiang et al., 2008; Moutinho & Landreth, 2017; Riddell et al., 2007; T. Vanmierlo et al., 2011). As the cholesterol efflux capacity mediated by ABCA1 and ABCG1 was found to be impaired in individuals with AD and with mild cognitive impairment (Marchi et al., 2019; Turri et al., 2023; Yassine et al., 2016), promoting cholesterol efflux by 22-ketositosterol administration may have therapeutic potential.

In accordance with the strictly regulated cholesterol homeostasis in the brain, 22-ketositosterol administration did not affect the cholesterol concentration in the brain. However, in line with the previously reported differential regulation of the cholesterol metabolism in the brain of WT and AD mice, the cholesterol synthesis rate in WT mice, but not in APPswePS1ΔE9 mice, seemed to be decreased upon 22-ketositosterol treatment, as suggested by a decrease in the ratios of cholesterol precursors to cholesterol in WT mice exclusively (Vanmierlo et al., 2010). Providing an LXR agonist is expected to increase cholesterol turnover, as was seen with a synthetic LXR agonist (Vanmierlo et al., 2011). However, this was not observed with 22-ketositosterol. In contrast, the increase in the ratio of desmosterol/cholesterol in the liver upon 22-ketositosterol supplementation is suggestive of enhanced cholesterol synthesis. However, it could also be attributed to the observed decrease in the hepatic cholesterol concentration as a result of an enhanced cholesterol secretion or an increased conversion into metabolites. The promotion of the conversion of cholesterol to 7 α -OHC, the rate-limiting step in the classic neutral pathway of formation of bile acids, is suggested by the elevated 7 α -OHC/cholesterol in the liver of 22-ketositosterol-supplemented animals. In addition, oxysterols such as 22-ketositosterol have been demonstrated to inhibit the activity of SREBPs and can thereby reduce the lipogenic pathway, for example, the synthesis of lipids and cholesterol (Radhakrishnan et al., 2004). Alternatively, the liver cholesterol concentrations may be decreased as a result of reduced intestinal sterol absorption, as indicated by the decreased campesterol/cholesterol ratio. Additionally, 22-ketositosterol may promote sterol excretion by LXR-mediated up-regulation of Abcg5/8 (Kruit et al., 2005; Yu et al., 2003). These cholesterol-lowering properties of 22-ketositosterol have the potential to prevent or restrict hypercholesterolemia and its associated conditions.

Pan LXR agonists are known to negatively affect the lipid profile leading to hepatosteatosis and hypertriglyceridemia (Grefhorst et al., 2002; Repa et al., 2000; Schultz et al., 2000). These adverse effects have been attributed to the activation of LXR α (Quinet et al., 2006; Schultz et al., 2000; Zhang et al., 2012) and linked to the up-regulation of LXR α target gene G0/G1 Switch Gene 2 (G0S2) leading to an inhibition of intracellular TG hydrolysis (Heckmann et al., 2017). The treatment of *Nr1h3*^{-/-} (LXR α gene) mice with synthetic LXR agonist **GW3965** has been shown to promote cholesterol efflux via activation of LXR β without inducing hepatosteatosis or hypertriglyceridemia (Bradley et al., 2007). In line with these results, a preferential LXR β agonist was demonstrated to increase the protein levels of apolipoprotein E (ApoE) in the brain of Tg2576 mice and rhesus monkeys without affecting hepatic triglyceride concentrations (Stachel et al., 2016). Therefore, compounds selectively activating LXR β may provide opportunities for application in AD treatment. 22-Ketositosterol was previously identified as a preferential activator of LXR β (PFM018 in Marinozzi et al., 2017). Although 22-ketositosterol activated LXR β slightly more than LXR α in CCF-STTG1 cells, which was in accordance with the results of pan LXR agonist T0901317, we demonstrate a comparable activation of LXR α and LXR β in HEK293, SH-SY5Y and CHME3 cells. The disparity in the findings reported in this study and those previously documented by Marinozzi et al. could stem from differences in the reporter assays used. Marinozzi et al. used a luciferase assay with GAL-4 chimeric receptors assessing mostly binding of the compounds to LXR α and LXR β (Marinozzi et al., 2017), while we determined the transcriptional activation of LXR in luciferase reporter assays by transfecting cells with pcDNA3.1/V5H6 vector containing clones of the full-length cDNAs for the murine nuclear receptors LXR α or LXR β and vectors encoding RXR α and LXRE (Zwarts et al., 2019). Although we could not confirm the strong preference of 22-ketositosterol for LXR β , no lipid accumulation was induced in the liver or serum after diet supplementation with 22-ketositosterol in mice. It is unlikely that this results from 22-ketositosterol being a highly selective LXR β agonist. More likely is the involvement of LXR-independent effects, such as SREBP1 inhibition as demonstrated for oxysterols (Radhakrishnan et al., 2004), which may counteract LXR α -induced lipogenesis. In line, 22-ketositosterol did not increase the expression of *SREBF1* or its target genes *FASN*, *ACACA* and *SCD1*. Instead, *ACACA* expression even demonstrated a slight reduction upon 22-ketositosterol supplementation. In addition, no treatment effect was detected on the expression of LXR α -responsive gene *G0S2* of which an up-regulation is believed to contribute to the adverse effects of LXR α activation on lipid accumulation (Heckmann et al., 2017). 22-Ketositosterol could therefore serve as a safe therapeutic agent, even though activating both LXR α and LXR β .

5 | CONCLUSION

Our data suggest that LXR-activating 22-ketositosterol has potential therapeutic beneficial effects in the context of neurodegenerative

conditions such as AD. It may prevent disease progression by promoting cholesterol efflux and possibly by mitigating AD-related neuro-inflammatory processes. Considering that 22-ketositosterol stands out for not inducing lipid accumulation in the liver or serum, unlike other synthetic LXR agonists, further investigation into its potential therapeutic application in diseases that could benefit from dampening inflammation and enhancing cholesterol efflux is warranted.

AUTHOR CONTRIBUTIONS

Conceptualisation: Monique T Mulder, Tim Vanmierlo, Johan W Jonker, Folkert Kuipers and Dieter Lütjohann. **Methodology:** Nikita Martens, Monique T Mulder, Tim Vanmierlo, Johan W Jonker, Folkert Kuipers, Dieter Lütjohann and Maura Marinozzi. **Validation:** Nikita Martens, Na Zhan, Sammie C Yam, Marcella Palumbo, Lorenzo Pontini, Frank P J Leijten, Leonie van Vark-van der Zee and Silvia Friedrichs. **Formal Analysis:** Nikita Martens, Monique T Mulder and Tim Vanmierlo. **Investigation:** Nikita Martens, Na Zhan, Sammie C Yam, Marcella Palumbo, Lorenzo Pontini, Frank P J Leijten, Leonie van Vark-van der Zee, Gardi Voortman, Silvia Friedrichs and Albert Gerdig. **Resources:** Monique T Mulder, Tim Vanmierlo, Johan W Jonker, Folkert Kuipers and Dieter Lütjohann. **Writing – Original Draft:** Nikita Martens and Monique T Mulder; **Writing – Review and Editing:** All authors. **Visualisation:** Nikita Martens, Na Zhan and Sammie C Yam. **Supervision:** Monique T Mulder and Tim Vanmierlo. **Project Administration:** Nikita Martens, Na Zhan, Monique T Mulder, Tim Vanmierlo and Dieter Lütjohann. **Funding Acquisition:** Monique T Mulder, Tim Vanmierlo, Johan W Jonker, Folkert Kuipers and Dieter Lütjohann.

ACKNOWLEDGEMENTS

This work was supported by NextGenerationEU (NGEU). This research was funded by the Dutch Research Council (NWO-TTW; #16437), the Alzheimer Nederland and Alzheimer Forschung Initiative (#WE.03-2022-06, #WE.15-2021-08, #AFI-22034CB) and the Ministry of University and Research (MUR), National Recovery and Resilience Plan (NRRP), project MNESYS (PE0000006). We thank Dr. Adrie Verhoeven for providing feedback on the manuscript. The research was not preregistered with an analysis plan.

CONFLICT OF INTEREST STATEMENT

The authors declare that they have no conflicts of interest. The funders had no role in the design of the study; in the collection, analysis, or interpretation of data; or in the writing of the manuscript.

DATA AVAILABILITY STATEMENT

The data that support the findings of this study are available from the corresponding author upon reasonable request.

DECLARATION OF TRANSPARENCY AND SCIENTIFIC RIGOUR

This Declaration acknowledges that this paper adheres to the principles for transparent reporting and scientific rigour of preclinical research as stated in the *BJP* guidelines for [Design & Analysis](#),

[Immunoblotting and Immunochemistry](#) and [Animal Experimentation](#), and as recommended by funding agencies, publishers and other organisations engaged with supporting research. The research was not preregistered.

ORCID

Nikita Martens  <https://orcid.org/0000-0001-6382-3379>

Maura Marinozzi  <https://orcid.org/0000-0001-5994-9390>

Dieter Lütjohann  <https://orcid.org/0000-0002-7941-8308>

REFERENCES

- Adorni, M. P., Papotti, B., Borghi, M. O., Raschi, E., Zimetti, F., Bernini, F., Meroni, P. L., & Ronda, N. (2023). Effect of the JAK/STAT inhibitor tofacitinib on macrophage cholesterol metabolism. *International Journal of Molecular Sciences*, 24(16), 12571. <https://doi.org/10.3390/ijms241612571>
- Alexander, S. P. H., Cidlowski, J. A., Kelly, E., Mathie, A. A., Peters, J. A., Veale, E. L., Armstrong, J. F., Faccenda, E., Harding, S. D., Davies, J. A., Coons, L., Fuller, P. J., Korach, K. S., & Young, M. J. (2023). The concise guide to PHARMACOLOGY 2023/24: Nuclear hormone receptors. *British Journal of Pharmacology*, 180(Suppl 2), S223–S240. <https://doi.org/10.1111/bph.16179>
- Alexander, S. P. H., Roberts, R. E., Broughton, B. R. S., Sobey, C. G., George, C. H., Stanford, S. C., Cirino, G., Docherty, J. R., Giembycz, M. A., Hoyer, D., Insel, P. A., Izzo, A. A., Ji, Y., MacEwan, D. J., Mangum, J., Wonnacott, S., & Ahluwalia, A. (2018). Goals and practicalities of immunoblotting and immunohistochemistry: A guide for submission to the British Journal of Pharmacology. *British Journal of Pharmacology*, 175(3), 407–411. <https://doi.org/10.1111/bph.14112>
- Arganda-Carreras, I., Kaynig, V., Rueden, C., Eliceiri, K. W., Schindelin, J., Cardona, A., & Sebastian Seung, H. (2017). Trainable Weka segmentation: A machine learning tool for microscopy pixel classification. *Bioinformatics*, 33(15), 2424–2426. <https://doi.org/10.1093/bioinformatics/btx180>
- Bai, W., Liu, T., Yi, H., Li, S., & Tian, X. (2012). Anticipatory activity in rat medial prefrontal cortex during a working memory task. *Neuroscience Bulletin*, 28(6), 693–703. <https://doi.org/10.1007/s12264-012-1291-x>
- Berghoff, S. A., Spieth, L., Sun, T., Hosang, L., Schlaphoff, L., Depp, C., Dükling, T., Winchenbach, J., Neuber, J., Ewers, D., Scholz, P., van der Meer, F., Cantuti-Castelvetri, L., Sasmita, A. O., Meschkat, M., Ruhwedel, T., Möbius, W., Sankowski, R., Prinz, M., ... Saher, G. (2021). Microglia facilitate repair of demyelinated lesions via post-squalene sterol synthesis. *Nature Neuroscience*, 24(1), 47–60. <https://doi.org/10.1038/s41593-020-00757-6>
- Blennow, K., de Leon, M. J., & Zetterberg, H. (2006). Alzheimer's disease. *Lancet*, 368(9533), 387–403. [https://doi.org/10.1016/S0140-6736\(06\)69113-7](https://doi.org/10.1016/S0140-6736(06)69113-7)
- Bligh, E. G., & Dyer, W. J. (1959). A rapid method of total lipid extraction and purification. *Canadian Journal of Biochemistry and Physiology*, 37(8), 911–917. <https://doi.org/10.1139/o59-099>
- Bogie, J., Hoeks, C., Schepers, M., Tiane, A., Cuypers, A., Leijten, F., Chintapakorn, Y., Suttiyut, T., Pornpakakul, S., Struik, D., Kerk siek, A., Liu, H. B., Hellings, N., Martinez-Martinez, P., Jonker, J. W., Dewachter, I., Sijbrands, E., Walter, J., Hendriks, J., ... Mulder, M. (2019). Dietary Sargassum fusiforme improves memory and reduces amyloid plaque load in an Alzheimer's disease mouse model. *Scientific Reports*, 9(1), 4908. <https://doi.org/10.1038/s41598-019-41399-4>
- Bradley, M. N., Hong, C., Chen, M., Joseph, S. B., Wilpitz, D. C., Wang, X., Lusis, A. J., Collins, A., Hseuh, W. A., Collins, J. L., Tangirala, R. K., & Tontonoz, P. (2007). Ligand activation of LXR beta reverses atherosclerosis and cellular cholesterol overload in mice lacking LXR alpha and apoE. *The Journal of Clinical Investigation*, 117(8), 2337–2346.

- Cantuti-Castelvetri, L., Fitzner, D., Bosch-Queralt, M., Weil, M. T., Su, M., Sen, P., Ruhwedel, T., Mitkovski, M., Trendelenburg, G., Lütjohann, D., Möbius, W., & Simons, M. (2018). Defective cholesterol clearance limits remyelination in the aged central nervous system. *Science*, 359(6376), 684–688. <https://doi.org/10.1126/science.aan4183>
- Chistiakov, D. A., Killingsworth, M. C., Myasoedova, V. A., Orekhov, A. N., & Bobryshev, Y. V. (2017). CD68/macrosialin: Not just a histochemical marker. *Laboratory Investigation*, 97(1), 4–13. <https://doi.org/10.1038/labinvest.2016.116>
- Curtis, M. J., Alexander, S. P. H., Cirino, G., George, C. H., Kendall, D. A., Insel, P. A., Izzo, A. A., Ji, Y., Panettieri, R. A., Patel, H. H., Sobey, C. G., Stanford, S. C., Stanley, P., Stefanska, B., Stephens, G. J., Teixeira, M. M., Vergnolle, N., & Ahluwalia, A. (2022). Planning experiments: Updated guidance on experimental design and analysis and their reporting III. *British Journal of Pharmacology*, 179, 3907–3913. <https://doi.org/10.1111/bph.15868>
- Dixon, W. J. (1950). Analysis of extreme values. *The Annals of Mathematical Statistics*, 21(4), 488–506.
- Dixon, W. J. (1951). Ratios involving extreme values. *The Annals of Mathematical Statistics*, 22(1), 68–78. <https://doi.org/10.1214/aoms/1177729693>
- Donkin, J. J., Stukas, S., Hirsch-Reinshagen, V., Namjoshi, D., Wilkinson, A., May, S., Chan, J., Fan, J., Collins, J., & Wellington, C. L. (2010). ATP-binding cassette transporter A1 mediates the beneficial effects of the liver X receptor agonist GW3965 on object recognition memory and amyloid burden in amyloid precursor protein/presenilin 1 mice. *The Journal of Biological Chemistry*, 285(44), 34144–34154. <https://doi.org/10.1074/jbc.M110.108100>
- Fedoseienko, A., Wijers, M., Wolters, J. C., Dekker, D., Smit, M., Huijckman, N., Kloosterhuis, N., Klug, H., Schepers, A., Willems van Dijk, K., Levels, J. H. M., Billadeau, D. D., Hofker, M. H., van Deursen, J., Westerterp, M., Burstein, E., Kuivenhoven, J. A., & van de Sluis, B. (2018). The COMMD family regulates plasma LDL Levels and attenuates atherosclerosis through stabilizing the CCC complex in endosomal LDLR trafficking. *Circulation Research*, 122(12), 1648–1660. <https://doi.org/10.1161/CIRCRESAHA.117.312004>
- Grefhorst, A., Elzinga, B. M., Voshol, P. J., Plösch, T., Kok, T., Bloks, V. W., van der Sluijs, F. H., Havekes, L. M., Romijn, J. A., Verkade, H. J., & Kuipers, F. (2002). Stimulation of lipogenesis by pharmacological activation of the liver X receptor leads to production of large, triglyceride-rich very low density lipoprotein particles. *The Journal of Biological Chemistry*, 277(37), 34182–34190. <https://doi.org/10.1074/jbc.M204887200>
- Hardy, J., & Selkoe, D. J. (2002). The amyloid hypothesis of Alzheimer's disease: Progress and problems on the road to therapeutics. *Science*, 297(5580), 353–356.
- Heckmann, B. L., Zhang, X., Saarinen, A. M., Schoiswohl, G., Kershaw, E. E., Zechner, R., & Liu, J. (2017). Liver X receptor α mediates hepatic triglyceride accumulation through upregulation of G0/G1 switch gene 2 expression. *JCI Insight*, 2(4), e88735. <https://doi.org/10.1172/jci.insight.88735>
- Heneka, M. T., Carson, M. J., El Khoury, J., Landreth, G. E., Brosseron, F., Feinstein, D. L., Jacobs, A. H., Wyss-Coray, T., Vitorica, J., Ransohoff, R. M., Herrup, K., Frautschy, S. A., Finsen, B., Brown, G. C., Verkhratsky, A., Yamanaka, K., Koistinaho, J., Latz, E., Halle, A., ... Kummer, M. P. (2015). Neuroinflammation in Alzheimer's disease. *Lancet Neurology*, 14(4), 388–405.
- Jiang, Q., Lee, C. Y., Mandrekar, S., Wilkinson, B., Cramer, P., Zelcer, N., Mann, K., Lamb, B., Willson, T. M., Collins, J. L., Richardson, J. C., Smith, J. D., Comery, T. A., Riddell, D., Holtzman, D. M., Tontonoz, P., & Landreth, G. E. (2008). ApoE promotes the proteolytic degradation of Abeta. *Neuron*, 58(5), 681–693. <https://doi.org/10.1016/j.neuron.2008.04.010>
- Kruit, J. K., Plösch, T., Havinga, R., Boverhof, R., Groot, P. H., Groen, A. K., & Kuipers, F. (2005). Increased fecal neutral sterol loss upon liver X receptor activation is independent of biliary sterol secretion in mice. *Gastroenterology*, 128(1), 147–156. <https://doi.org/10.1053/j.gastro.2004.10.006>
- Larsen, L. E., van den Boogert, M. A. W., Rios-Ocampo, W. A., Jansen, J. C., Conlon, D., Chong, P. L. E., Levels, J. H. M., Eilers, R. E., Sachdev, V. V., Zelcer, N., Raabe, T., He, M., Hand, N. J., Drenth, J. P. H., Rader, D. J., Stroes, E. S. G., Lefeber, D. J., Jonker, J. W., & Holleboom, A. G. (2022). Defective lipid droplet-lysosome interaction causes fatty liver disease as evidenced by human mutations in TMEM199 and CCDC115. *Cellular and Molecular Gastroenterology and Hepatology*, 13(2), 583–597. <https://doi.org/10.1016/j.jcmgh.2021.09.013>
- Lee, M. S., & Bensinger, S. J. (2022). Reprogramming cholesterol metabolism in macrophages and its role in host defense against cholesterol-dependent cytotoxicity. *Cellular & Molecular Immunology*, 19(3), 327–336. <https://doi.org/10.1038/s41423-021-00827-0>
- Lilley, E., Stanford, S. C., Kendall, D. E., Alexander, S. P. H., Cirino, G., Docherty, J. R., George, C. H., Insel, P. A., Izzo, A. A., Ji, Y., Panettieri, R. A., Sobey, C. G., Stefanska, B., Stephens, G., Teixeira, M., & Ahluwalia, A. (2020). ARRIVE 2.0 and the British Journal of Pharmacology: Updated guidance for 2020. *British Journal of Pharmacology*, 177(16), 3611–3616. <https://doi.org/10.1111/BPH.15178>
- Lütjohann, D., Brzezinka, A., Barth, E., Abramowski, D., Staufenbiel, M., von Bergmann, K., Beyreuther, K., Multhaup, G., & Bayer, T. A. (2002). Profile of cholesterol-related sterols in aged amyloid precursor protein transgenic mouse brain. *Journal of Lipid Research*, 43(7), 1078–1085.
- Mackay, D. S., Jones, P. J., Myrie, S. B., Plat, J., & Lütjohann, D. (2014). Methodological considerations for the harmonization of non-cholesterol sterol bio-analysis. *Journal of Chromatography. B, Analytical Technologies in the Biomedical and Life Sciences*, 957, 116–122. <https://doi.org/10.1016/j.jchromb.2014.02.052>
- Marchi, C., Adorni, M. P., Caffarra, P., Ronda, N., Spallazzi, M., Barocco, F., Galimberti, D., Bernini, F., & Zimetti, F. (2019). ABCA1- and ABCG1-mediated cholesterol efflux capacity of cerebrospinal fluid is impaired in Alzheimer's disease. *Journal of Lipid Research*, 60(8), 1449–1456. <https://doi.org/10.1194/jlr.P091033>
- Marinozzi, M., Castro Navas, F. F., Maggioni, D., Carosati, E., Bocci, G., Carloncelli, M., Giorgi, G., Cruciani, G., Fontana, R., & Russo, V. (2017). Side-chain modified ergosterol and stigmasterol derivatives as liver X receptor agonists. *Journal of Medicinal Chemistry*, 60(15), 6548–6562. <https://doi.org/10.1021/acs.jmedchem.7b00091>
- Martens, N., Schepers, M., Zhan, N., Leijten, F., Voortman, G., Tiane, A., Rombaut, B., Poisquet, J., Sande, N. V., Kerk siek, A., Kuipers, F., Jonker, J. W., Liu, H., Lütjohann, D., Vanmierlo, T., & Mulder, M. T. (2021). 24(S)-Saringosterol prevents cognitive decline in a mouse model for Alzheimer's disease. *Marine Drugs*, 19(4), 190. <https://doi.org/10.3390/md19040190>
- Martens, N., Zhan, N., Yam, S. C., Leijten, F. P. J., Palumbo, M., Caspers, M., Tiane, A., Friedrichs, S., Li, Y., van Vark-van der Zee, L., Voortman, G., Zimetti, F., Jaarsma, D., Verschuren, L., Jonker, J. W., Kuipers, F., Lütjohann, D., Vanmierlo, T., & Mulder, M. T. (2024). Supplementation of seaweed extracts to the diet reduces symptoms of Alzheimer's disease in the APPswePS1 Δ E9 mouse model. *Nutrients*, 16(11), 1614. <https://doi.org/10.3390/nu16111614>
- McDonnell, D. P., & Safi, R. (2023). 1H. Liver X receptor-like receptors in GtoPdb v. 2023.1. *IUPHAR/BPS Guide to Pharmacology CITE*, 2023(1). <https://doi.org/10.2218/gtopdb/F89/2023.1>
- Moutinho, M., & Landreth, G. E. (2017). Therapeutic potential of nuclear receptor agonists in Alzheimer's disease. *Journal of Lipid Research*, 58(10), 1937–1949. <https://doi.org/10.1194/jlr.R075556>
- Mouzat, K., Chudinova, A., Polge, A., Kantar, J., Camu, W., Raoul, C., & Lumbroso, S. (2019). Regulation of brain cholesterol: What role do liver X receptors play in neurodegenerative diseases? *International Journal of Molecular Sciences*, 20(16), 3858. <https://doi.org/10.3390/ijms20163858>
- Percie du Sert, N., Hurst, V., Ahluwalia, A., Alam, S., Avey, M. T., Baker, M., Browne, W. J., Clark, A., Cuthill, I. C., Dirnagl, U., Emerson, M., Garner, P., Holgate, S. T., Howells, D. W., Karp, N. A., Lazic, S. E.,

- Lidster, K., MacCallum, C. J., Macleod, M., ... Würbel, H. (2020). The ARRIVE guidelines 2.0: updated guidelines for reporting animal research. *PLoS Biology*, 18(7), e3000410. <https://doi.org/10.1371/journal.pbio.3000410>
- Quinet, E. M., Savio, D. A., Halpern, A. R., Chen, L., Schuster, G. U., Gustafsson, J. A., Basso, M. D., & Nambi, P. (2006). Liver X receptor (LXR)-beta regulation in LXRalpha-deficient mice: Implications for therapeutic targeting. *Molecular Pharmacology*, 70(4), 1340–1349. <https://doi.org/10.1124/mol.106.022608>
- Radhakrishnan, A., Sun, L. P., Kwon, H. J., Brown, M. S., & Goldstein, J. L. (2004). Direct binding of cholesterol to the purified membrane region of SCAP: Mechanism for a sterol-sensing domain. *Molecular Cell*, 15(2), 259–268. <https://doi.org/10.1016/j.molcel.2004.06.019>
- Repa, J. J., Liang, G., Ou, J., Bashmakov, Y., Lobaccaro, J. M., Shimomura, I., Shan, B., Brown, M. S., Goldstein, J. L., & Mangelsdorf, D. J. (2000). Regulation of mouse sterol regulatory element-binding protein-1c gene (SREBP-1c) by oxysterol receptors, LXRalpha and LXRbeta. *Genes & Development*, 14(22), 2819–2830. <https://doi.org/10.1101/gad.844900>
- Riddell, D. R., Zhou, H., Comery, T. A., Kouranova, E., Lo, C. F., Warwick, H. K., Ring, R. H., Kirksey, Y., Aschmies, S., Xu, J., Kubek, K., Hirst, W. D., Gonzales, C., Chen, Y., Murphy, E., Leonard, S., Vasylyev, D., Oganessian, A., Martone, R. L., ... Jacobsen, J. S. (2007). The LXR agonist TO901317 selectively lowers hippocampal Abeta42 and improves memory in the Tg2576 mouse model of Alzheimer's disease. *Molecular and Cellular Neurosciences*, 34(4), 621–628.
- Sandoval-Hernández, A. G., Buitrago, L., Moreno, H., Cardona-Gómez, G. P., & Arboleda, G. (2015). Role of liver X receptor in AD pathophysiology. *PLoS ONE*, 10(12), e0145467. <https://doi.org/10.1371/journal.pone.0145467>
- Schultz, J. R., Tu, H., Luk, A., Repa, J. J., Medina, J. C., Li, L., Schwendner, S., Wang, S., Thoolen, M., Mangelsdorf, D. J., Lustig, K. D., & Shan, B. (2000). Role of LXRs in control of lipogenesis. *Genes & Development*, 14(22), 2831–2838. <https://doi.org/10.1101/gad.850400>
- Stachel, S. J., Zerbinatti, C., Rudd, M. T., Cosden, M., Suon, S., Nanda, K. K., Wessner, K., DiMuzio, J., Maxwell, J., Wu, Z., Uslaner, J. M., Michener, M. S., Szczerba, P., Brnardic, E., Rada, V., Kim, Y., Meissner, R., Wuelfing, P., Yuan, Y., ... Renger, J. (2016). Identification and in vivo evaluation of liver X receptor β -selective agonists for the potential treatment of Alzheimer's disease. *Journal of Medicinal Chemistry*, 59(7), 3489–3498. <https://doi.org/10.1021/acs.jmedchem.6b00176>
- Turri, M., Conti, E., Pavanello, C., Gastoldi, F., Palumbo, M., Bernini, F., Aprea, V., Re, F., Barbiroli, A., Emide, D., Galimberti, D., Tremolizzo, L., Zimetti, F., Calabresi, L., & Group, A.-A. (2023). Plasma and cerebrospinal fluid cholesterol esterification is hampered in Alzheimer's disease. *Alzheimer's Research & Therapy*, 15(1), 95. <https://doi.org/10.1186/s13195-023-01241-6>
- Vanmierlo, T., Bloks, V. W., van Vark-van der Zee, L. C., Rutten, K., Kerksiek, A., Friedrichs, S., Sijbrands, E., Steinbusch, H. W., Kuipers, F., Lütjohann, D., & Mulder, M. (2010). Alterations in brain cholesterol metabolism in the APPSLxPS1mut mouse, a model for Alzheimer's disease. *Journal of Alzheimer's Disease*, 19(1), 117–127. <https://doi.org/10.3233/JAD-2010-1209>
- Vanmierlo, T., Rutten, K., Dederen, J., Bloks, V. W., Kuipers, F., Kiliaan, A., Blokland, A., Sijbrands, E. J., Steinbusch, H., & Prickaerts, J. (2011). Liver X receptor activation restores memory in aged AD mice without reducing amyloid. *Neurobiology of Aging*, 32(7), 1262–1272. <https://doi.org/10.1016/j.neurobiolaging.2009.07.005>
- Vogel-Ciernia, A., & Wood, M. A. (2014). Examining object location and object recognition memory in mice. *Current Protocols in Neuroscience*, 69, 8–31.
- Westerterp, M., Fotakis, P., Ouimet, M., Bochem, A. E., Zhang, H., Molusky, M. M., Wang, W., Abramowicz, S., la Bastide-van Gemert, S., Wang, N., Welch, C. L., Reilly, M. P., Stroes, E. S., Moore, K. J., & Tall, A. R. (2018). Cholesterol efflux pathways suppress inflammasome activation, NETosis, and atherogenesis. *Circulation*, 138(9), 898–912. <https://doi.org/10.1161/CIRCULATIONAHA.117.032636>
- Xu, X., Xiao, X., Yan, Y., & Zhang, T. (2021). Activation of liver X receptors prevents emotional and cognitive dysfunction by suppressing microglial M1-polarization and restoring synaptic plasticity in the hippocampus of mice. *Brain, Behavior, and Immunity*, 94, 111–124. <https://doi.org/10.1016/j.bbi.2021.02.026>
- Yassine, H. N., Feng, Q., Chiang, J., Petrosspour, L. M., Fonteh, A. N., Chui, H. C., & Harrington, M. G. (2016). ABCA1-mediated cholesterol efflux capacity to cerebrospinal fluid is reduced in patients with mild cognitive impairment and Alzheimer's disease. *Journal of the American Heart Association*, 5(2), e002886.
- Yong, H. Y. F., Rawji, K. S., Ghorbani, S., Xue, M., & Yong, V. W. (2019). The benefits of neuroinflammation for the repair of the injured central nervous system. *Cellular & Molecular Immunology*, 16(6), 540–546. <https://doi.org/10.1038/s41423-019-0223-3>
- Yu, L., York, J., von Bergmann, K., Lütjohann, D., Cohen, J. C., & Hobbs, H. H. (2003). Stimulation of cholesterol excretion by the liver X receptor agonist requires ATP-binding cassette transporters G5 and G8. *The Journal of Biological Chemistry*, 278(18), 15565–15570.
- Zelcer, N., Khanlou, N., Clare, R., Jiang, Q., Reed-Geaghan, E. G., Landreth, G. E., Vinters, H. V., & Tontonoz, P. (2007). Attenuation of neuroinflammation and Alzheimer's disease pathology by liver X receptors. *Proceedings of the National Academy of Sciences*, 104(25), 10601–10606. <https://doi.org/10.1073/pnas.0701096104>
- Zelcer, N., & Tontonoz, P. (2006). Liver X receptors as integrators of metabolic and inflammatory signaling. *The Journal of Clinical Investigation*, 116(3), 607–614.
- Zhan, N., Wang, B., Martens, N., Liu, Y., Zhao, S., Voortman, G., van Rooij, J., Leijten, F., Vanmierlo, T., Kuipers, F., Jonker, J. W., Bloks, V. W., Lütjohann, D., Palumbo, M., Zimetti, F., Adorni, M. P., Liu, H., & Mulder, M. T. (2023). Identification of side chain oxidized sterols as novel liver X receptor agonists with therapeutic potential in the treatment of cardiovascular and neurodegenerative diseases. *International Journal of Molecular Sciences*, 24(2), 1290. <https://doi.org/10.3390/ijms24021290>
- Zhang, Y., Breevoort, S. R., Angdisen, J., Fu, M., Schmidt, D. R., Holmstrom, S. R., Kliever, S. A., Mangelsdorf, D. J., & Schulman, I. G. (2012). Liver LXR α expression is crucial for whole body cholesterol homeostasis and reverse cholesterol transport in mice. *The Journal of Clinical Investigation*, 122(5), 1688–1699. <https://doi.org/10.1172/JCI59817>
- Zwarts, I., van Zutphen, T., Kruit, J. K., Liu, W., Oosterveer, M. H., Verkade, H. J., Uhlenhaut, N. H., & Jonker, J. W. (2019). Identification of the fructose transporter GLUT5 (SLC2A5) as a novel target of nuclear receptor LXR. *Scientific Reports*, 9(1), 9299. <https://doi.org/10.1038/s41598-019-45803-x>

SUPPORTING INFORMATION

Additional supporting information can be found online in the Supporting Information section at the end of this article.

How to cite this article: Martens, N., Zhan, N., Yam, S. C., Palumbo, M., Pontini, L., Leijten, F. P. J., van Vark-van der Zee, L., Voortman, G., Friedrichs, S., Gerding, A., Marinuzzi, M., Jonker, J. W., Kuipers, F., Lütjohann, D., Vanmierlo, T., & Mulder, M. T. (2025). Role for the liver X receptor agonist 22-ketositosterol in preventing disease progression in an Alzheimer's disease mouse model. *British Journal of Pharmacology*, 1–23. <https://doi.org/10.1111/bph.70031>